THESIS/
REPORTS
Albini,
F.A.

TESTING AND EVALUATION OF A LARGE WOOD FUEL BURNOUT MODEL FOR FIRE EFFECTS AND FIRE DANGER RATING APPLICATIONS

FINAL REPORT FOR RESEARCH AGREEMENT
#INT-94947-RJVA
"Testing and Evaluation of a Large Woody Fuel Burnout Model for Fire Effects and Fire Danger Rating Applications"
MONTANA STATE UNIVERSITY
FS Contact: Dr. James K. Brown
CoOp Contact: Dr. Frank Albini

PERFORMANCE OF A LARGE FUEL BURNOUT MODEL IN FIRE DANGER RATING

Frank A. Albini
Adjunct Professor, Mechanical Engineering
Montana State University
Bozeman Montana 59717

22 February 1995

SUMMARY

The BURNUP computer model [Albini 1994a] was exercised using for surface fuel data the National Fire Danger Rating (NFDR) fuel model G [Burgan, Cohen, and Deeming 1977] and fire danger rating observations for 1993 and 1994 from NFDR station 240107 (Libby, Montana). These danger rating records were augmented by including the Canadian Duff Moisture Code and a duff moisture content inferred from this index [Canadian Forest Service Fire Danger Working Group 1987]. The surface fuel model was augmented by including a loading of duff sufficient to assure that it would be simulated to burn for the duration of all model exercises. The BURNUP model was used to simulate burning of large woody surface fuels and duff, and heat release per unit area was cumulated for a period of time following ignition to provide a measure of the heat load, or heat energy per unit area.

The exploratory investigations described here were to examine the possible use of BURNUP model predictions to supply an index equivalent to the NFDR Energy Release Component (ERC) that would admit of a more direct physical interpretation of its numerical value. This physical interpretation might render the quantity more valuable as an index of resistance to control and/or as a predictor of certain on-site fire effects related to the heat load. As a point of departure, the variation of the ERC index over the 1993 fire season is shown in figure 1and its behavior over a portion of the 1994 fire season in figure 2.

Using a constant ignition pulse of 50 kW/m^2 for 60 s and a fixed integration time of 9 min, starting after the ignition pulse, the heat load predictions shown in figures 3 and 4 were generated. These figures are to be compared to the ERC histories shown in figures 1 and 2. The rather "noisy" appearance of these predictions occurs because on some days the 1/4 - 1 inch fuel loading is ignited and on other days it is not. If this loading is ignited, then roughly the same amount of 1 - 3 inch and 3+ inch fuel is burned, according to the model. This is because the range of variation of the moisture contents of these larger fuel components is actually quite narrow. So the model predicts either a relatively large heat load or a small one. The gradual seasonal trend of the small heat load predictions is attributable to the duff moisture content variation. As the duff moisture content decreases, the rate of burning of the duff rises, yielding a larger heat load in the fixed integration time.

OBJECTIVES AND METHODS

The intent of this investigation was to explore use of the BURNUP model [Albini 1994a] to predict fire intensity (kW / m^2) as a function of time due to burning of the larger components of a fixed surface fuel accumulation in order to create a numerical index quantifying the potential heat load (MJ / m^2) as a function of the moisture contents of the various fuel size classes. Such an index would be expected to have a (relatively) small value if the large fuel elements were moist and a (relatively) large value when they were dry. By keeping records of the variation of such a parameter over the course of several years of wildland fire experience, one could then learn to interpret the numerical values in terms of conditions to be encountered in controlling wildfires and in terms of fire effects related to large fuel consumption and burning intensity. In mixed conifer forests of the Northern Rocky Mountains, the National Fire Danger Rating System index called the "Energy Release Component" [Burgan, Cohen, and Deeming 1977] computed for fuel model G (ERC-G), has been found to be a trustworthy index of this type. So a fire weather station in this region (Libby, Montana) was chosen as a trial site. The fire danger rating records for this station were processed for the 1993 fire season and for that portion of the 1994 fire season for which archival records were available at the time of this exercise.

Two issues had to be resolved before the BURNUP simulation model could be used in this manner:

(1) The igniting pulse of constant fire intensity for a finite duration that is demanded by the model had to be specified and

(2) The period of time over which to cumulate the simulated fire intensity had to be established.

In preliminary planning for this assessment exercise, possible methods of resolving these questions were explored. The simplest thing to do would be to use a constant ignition pulse intensity and duration, and a constant time period over which to cumulate simulated fire intensity. An invariant ignition pulse lacks realism in that it can lead to large simulated heat loads when the fine fuels are so moist that a fire cannot even be propagated. A constant integration time for fire intensity makes it questionable to use the simulated heat load in conjunction with fire spread rate to infer an edge intensity (or Byram's intensity), because the physical distances implied by the product of fire spread rate and the fixed integration time could become unrealistically large or small, depending upon the situation.

It was proposed to explore the inference of an ignition pulse from the burning of an "equivalent" single size class fuel bed derived by using an algorithm to be tested in the development of a second generation radiation-driven crown fire spread rate model [Albini 1994b]. This algorithm accepts an arbitrary collection of fuel components and combines them, conserving some features of the multicomponent fuel bed, into an equivalent uniform fuel bed of a single size class, moisture content, and intrinsic fuel particle properties. Using this single component fuel bed description, it is assumed that the entire fuel loading is burned at a steady rate during a constant intensity fire. The intensity of this hypothetical fire is found using the burning rate-vs-temperature [Albini and Reinhardt 1995] and temperature-vs-intensity [Albini et al, 1995] relationships incorporated in the BURNUP model. This algebra is described in appendix A.

It was decided to test a procedure for establishing a time interval for integration of the fire intensity that would reflect the tendency of an area fire to break into separate flaming zones of a size fixed by the average fire intensity (kW / m^2). A fundamental empirical finding of Heskestad [1991] was that if a fire burned at an average intensity I over a large area, it would tend to break into individual flame volumes of base dimension D, where

$$D = (I / G)^2 \quad ; \quad G = 53\ \mathrm{kW} / \mathrm{m}^{5/2} .$$

This relationship can be interpreted as a lean flammability limit. The more intense the fire, the larger can be the area that contributes to a single merged flame structure. By assuming that the base dimension in this equation is equal to the product of the spread rate and the time over which the time varying fire intensity is to be averaged, one can evaluate the integration time. The integration time derived in this manner is self-consistent in the sense that the fuel burned during this time period can be expected to contribute to a single flame structure whose base dimension is about as wide laterally as it is deep longitudinally. This algorithm is described in appendix B.

RESULTS

The ignition intensity pulse computation performed as expected. When the fine fuels are dry, they burn more rapidly, producing a more intense but shorter duration heat pulse. When they are moist, the igniting fire burns with less intensity for a longer period of time. But the variation predicted is not great, so in order to reflect the inability of a surface fire to spread in sufficiently moist fine fuels, it was necessary to introduce the "moisture of extinction" parameter [Burgan, Cohen, and Deeming 1977] to cause the predicted ignition pulse to decrease significantly as the fine fuel moisture approaches this cutoff value. But by doing so, the index of fire danger associated with the state of drying of the large fuels is made crucially sensitive to the moisture state of the fine fuels! In other words, the effort to model a "realistic" ignition pulse is counterproductive to the effort to generate an index reflecting the seasonal trend of the potential energy release by the large fuel components.

A similar perverse result occurs in the effort to establish a "consistent" time duration over which to cumulate the simulated fire intensity to create a measure of the heat load. Identical fire intensity histories that occur with different spread rate predictions (*e.g.*, under different wind speeds) will lead to different heat loads using this rationale for terminating the integral of intensity. The larger the spread rate, the smaller the heat load computed, as illustrated in figure 5. While this behavior of the index makes physical sense in terms of identifying the fuel that contributes to a single flame structure, it tends to makes the "large fuel index" sensitive to the predicted spread rate in a way that is not heuristically appealing. It tends to keep the heat load constant by shortening the integration period under conditions of rapid spread and lengthening it under conditions of marginal fire spread.

For these reasons, it appears that the simplest solution described above is probably the best one. If the ignition pulse is held fixed, the resulting simulated fire intensity history will reflect the dryness state of the larger fuel elements and the duff, and very little more. Likewise, if the integration time for cumulating the heat load is fixed, its value will not shift with the moisture content of the fine fuels or the wind speed, whose influence is measured by the NFDR spread index already.

The variation of predicted surface fire intensity (*i.e.*, not including the duff contribution) and cumulative heat pulse with time after ignition is shown in figure 6 for the fuel moisture conditions at Libby on 11 May 1993. This is day 41 on figures 1 and 3, near the early season maximum ERC. On this date, the ERC index is 37; it rises to a peak value of 42 seven days later and does not achieve that level again during the period plotted. The heat load cumulated over nine minutes after ignition is computed from the sum of the cumulative heat pulse of figure 6 at 540 seconds, plus the product of the duff burning intensity times the nine minute period. The heat load computed for these conditions (fig. 3) is 25.0 MJ / m^2 . The heat load peaks one day later, and stays between 25.0 and 25.5 for the next nine days.

For the fuel conditions of 2 August 1994 (day 94 on figures 2 and 4) the predicted surface fire intensity history and cumulative heat pulse are shown in figure 7. The ERC on this day is 68, a high not exceeded until day 105, when it reached a single reading of 70 for the period plotted in figure 2. The heat load computed for this day in the manner

described above is 26.6 MJ / m^2, a value only slightly above the 1993 peak, where the ERC was 42. The peak heat load for the plotted period occurred on day 105 at 27.9 MJ / m^2. Clearly there is not a one-to-one correspondence between the ERC and the heat load computed according to this paradigm.

As a point of reference, the surface fire intensity history for the limiting case when all fuel components, including the "live" fuel and duff, are absolutely bone dry, is shown in figure 8. The heat pulse from the surface fire, cumulated to 540 s, is about 30 MJ / m^2 , to which must be added the duff heat load that accrues during nine minutes, 6.0 MJ / m^2, for a total maximum heat load of about 36 MJ / m^2 for this fuel model.

Note that the peak heat load reached in 1994 is about 78% of this maximum value, while the 1993 maximum was about 71% of the maximum possible. So the heat load computed in this way tends to reach levels considerably higher, as a fraction of the maximum possible, than does the ERC for the same conditions. But the predicted heat load also tends to drop precipitously to zero, or near zero, under conditions which reduce only moderately the ERC index (compare especially figures 1 and 3).

SPECULATION ON MODEL REALISM

It is clear from the above comparison, limited though it is, that heat load predictions by the BURNUP simulation model will not serve as a substitute for the ERC, at least for NFDR fuel model G. The heat load predicted by the model is at once more sensitive to day-to-day swings in the fuel moisture contents and less sensitive to the slowly changing large fuel moisture contents than is the ERC algorithm currently used. The seasonal trends that accrue due to sustained periods of drying using the ERC index are not replicated by the heat load simulation.

This difference is due to the relative insensitivity of the simulation model predictions to the relatively small changes in moisture content of the largest fuel components. For example, the 1994 Libby data show the 100 hr and 1000 hr fuels at about 18% and 25% moisture content, respectively, on 1 May, the first day of data. On 2 August, these moistures reach data set minima of about 7% and 10% respectively. While these are indeed quite dry conditions that are indicative of high fire danger, the actual changes in fuel moisture content are not extreme. They are well within the range of the laboratory data used to calibrate the ignition delay and burning rate models used in the simulation and the "dry end" data are abundantly represented in the crib burns used to tune the predictions of burning rate through selection of the mixing ratio parameters that determine fire environment temperature as a function of intensity. In short, the simulation model should not be expected to predict drastic differences in burning rates for the larger fuel components under these moisture condition changes.

One problem in assessing the trend of wildland fire danger over a burning season is achieving a reflection of the growth in geographical area at risk to fire as the "dry zone" creeps up in elevation and widens in aspect range during the course of the summer season in midlatitude mountainous terrain. This poses a challenge to designers of algorithms for danger rating indices. Users of the NFDR system want a simple index that mimics this feature of seasonal variation. But if to get one they must observe and maintain records of phenological changes and weather conditions at different elevations and aspects, the activity of data gathering for fire danger rating can demand excessive time. For this reason it is desirable to have available an index that mimics the geographical effect as the season progresses but that does not demand much, if any, geographically related observations. The ERC, with the contribution of live fuel moisture content models, provides such a surrogate index. While it nominally gauges mostly the large surface fuel flammability by means of its moisture content variation, this physical interpretation of its meaning is at best weakly supported by laboratory and field data. Much of the appeal of ERC as an indicator of the level of fire danger stems from its success as a surrogate for the seasonal variation of the geographical area at

risk. From the exercises done to date using the BURNUP simulation model to compute a heat load, the predicted heat load will not perform this role. Whether or not the model provides an accurate prediction of the heat load that would occur given a fire on a particular day in the fuels specified by the fuel model used, it will not provide an index that varies seasonally in the same way that the ERC does. This does not mean that the heat load predicted is is necessarily wornq or right, but that the predicted value does not have the sensitivity to large fuel moisture content that renders the ERC a valuable fire danger rating planning tool.

FIGURE DESCRIPTIONS

Fig. 1 Seasonal variation of ERC at Libby, Montana for the 1993 fire season.

Fig. 2 Seasonal variation of ERC at Libby, Montana for early part of 1994 fire season.

Fig. 3 Seasonal variation at Libby, Montana for 1993 fire season of simulated heat load, including duff burning, for nine minutes following ignition of large surface fuels.

Fig. 4 Seasonal variation at Libby, Montana for early part of 1994 fire season of simulated heat load, including duff burning, for nine minutes following ignition of large surface fuels.

Fig. 5 Variation of heat load with fire intensity and spread rate, under the assumption that the fire creates a single flame structure with base dimension equal to the spread rate times the duration of the averaging time for intensity.

Fig. 6 Post-ignition fire intensity history and cumulative heat pulse for burning of surface fuels under conditions of 11 May 1993 at Libby, Montana.

Fig. 7 Post-ignition fire intensity history and cumulative heat pulse for burning of surface fuels under conditions of 2 Aug 1994 at Libby, Montana.

Fig. 8 Post-ignition fire intensity history and cumulative heat pulse for burning of surface fuels under limiting condition that all fuel components, including duff, have no moisture content whatsoever.

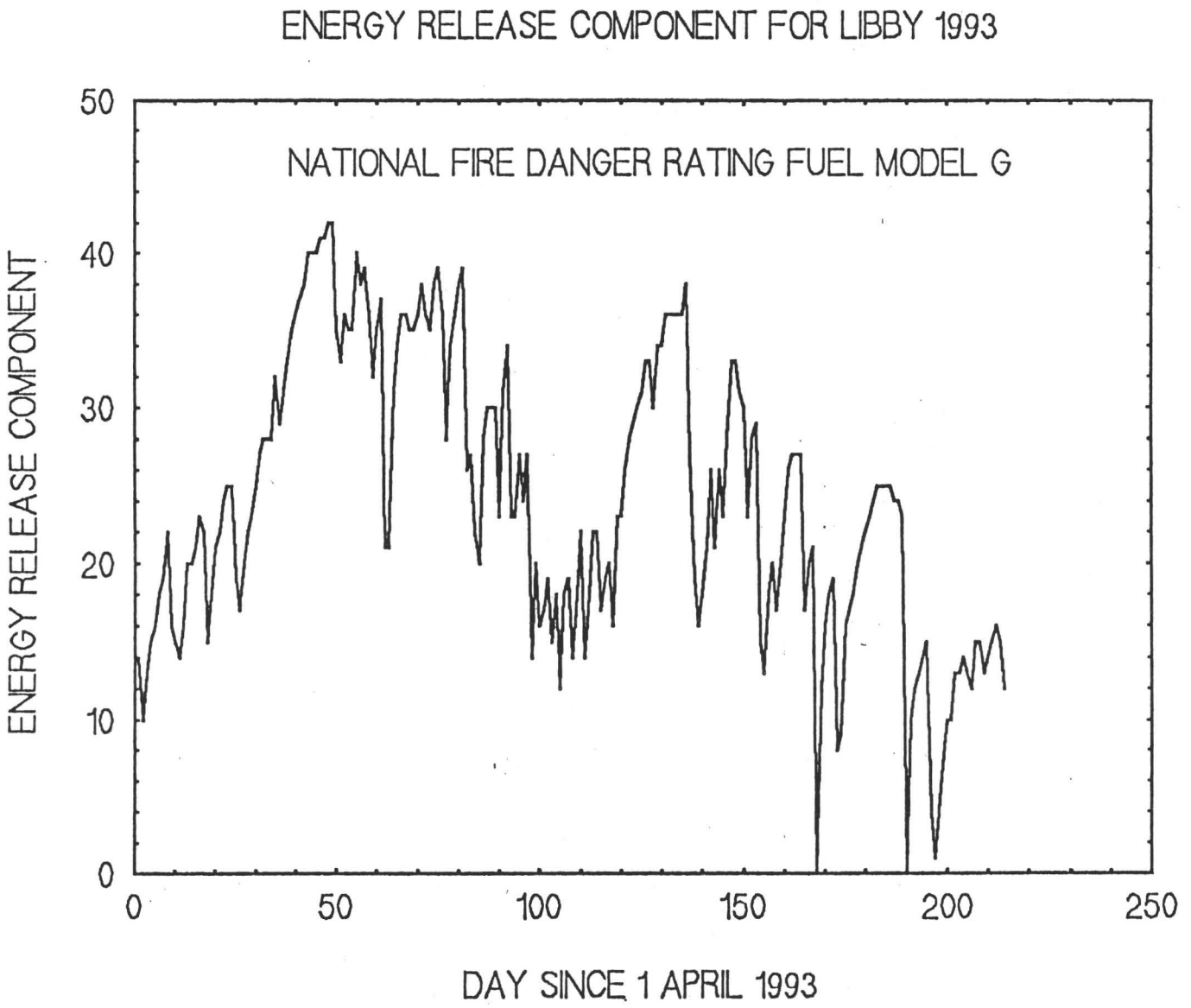

Fig. 1 Seasonal variation of ERC at Libby, Montana for the 1993 fire season.

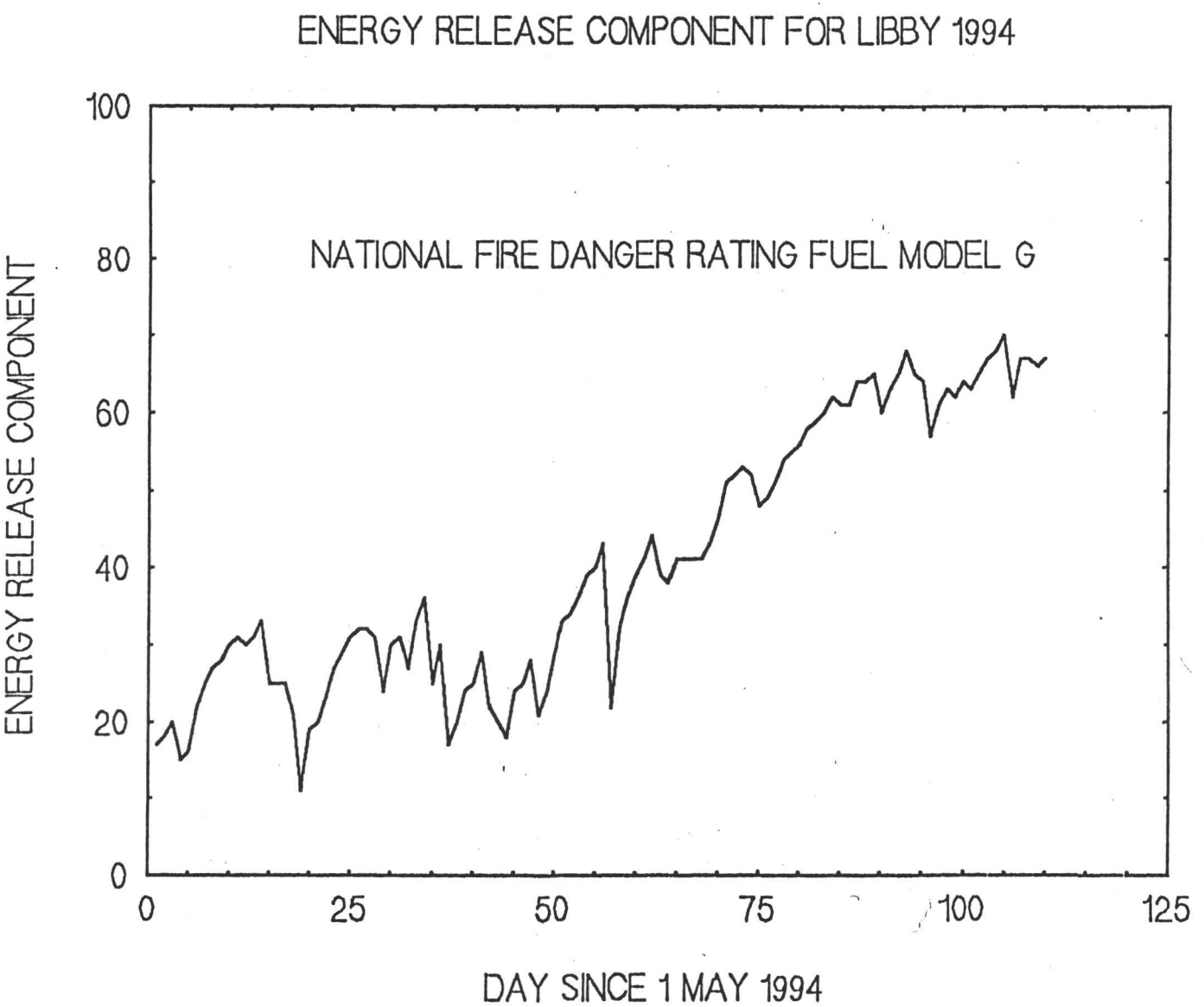

Fig. 2 Seasonal variation of ERC at Libby, Montana for early part of 1994 fire season.

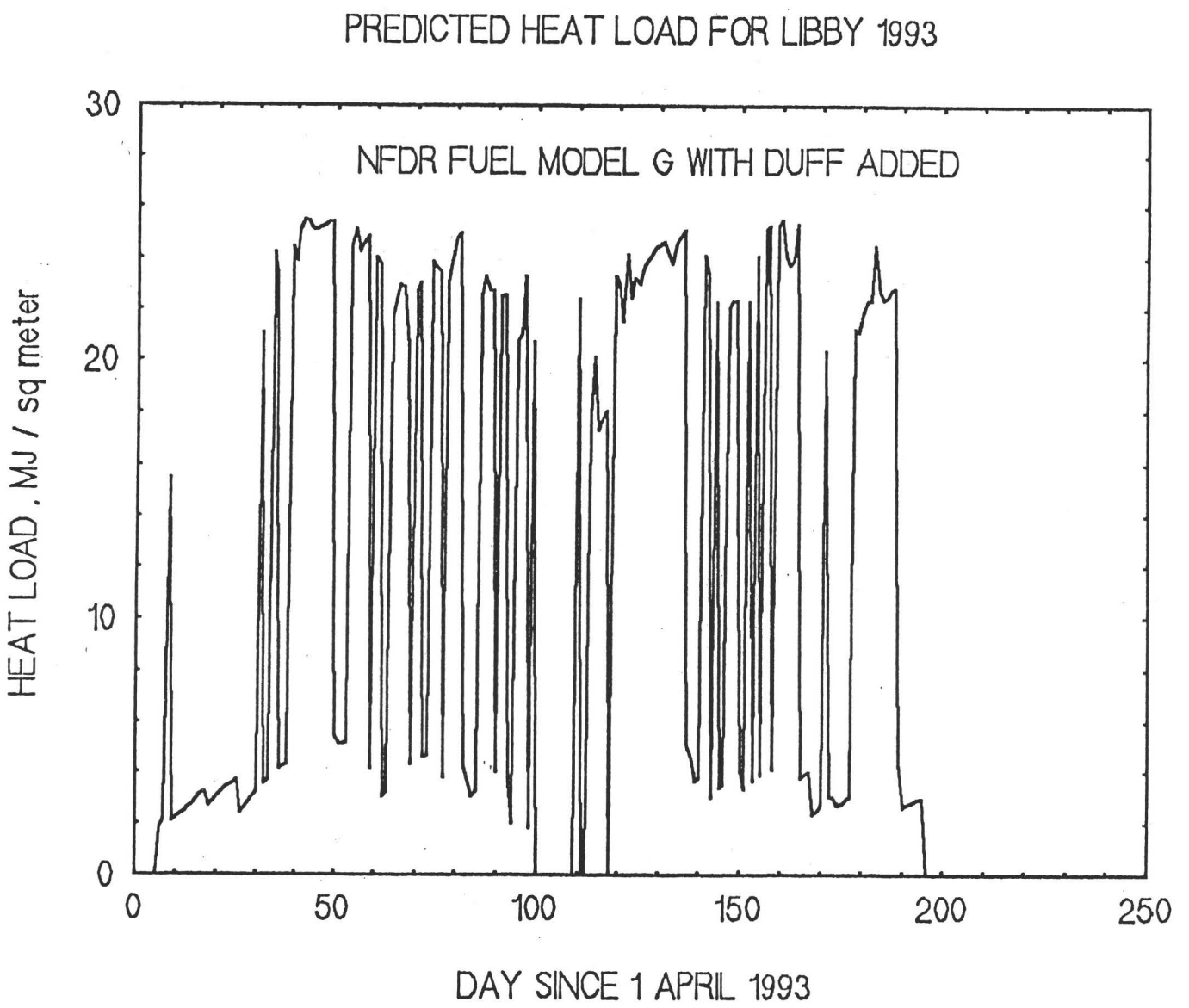

Fig. 3 Seasonal variation at Libby, Montana for 1993 fire season of simulated heat load, including duff burning, for nine minutes following ignition of large surface fuels.

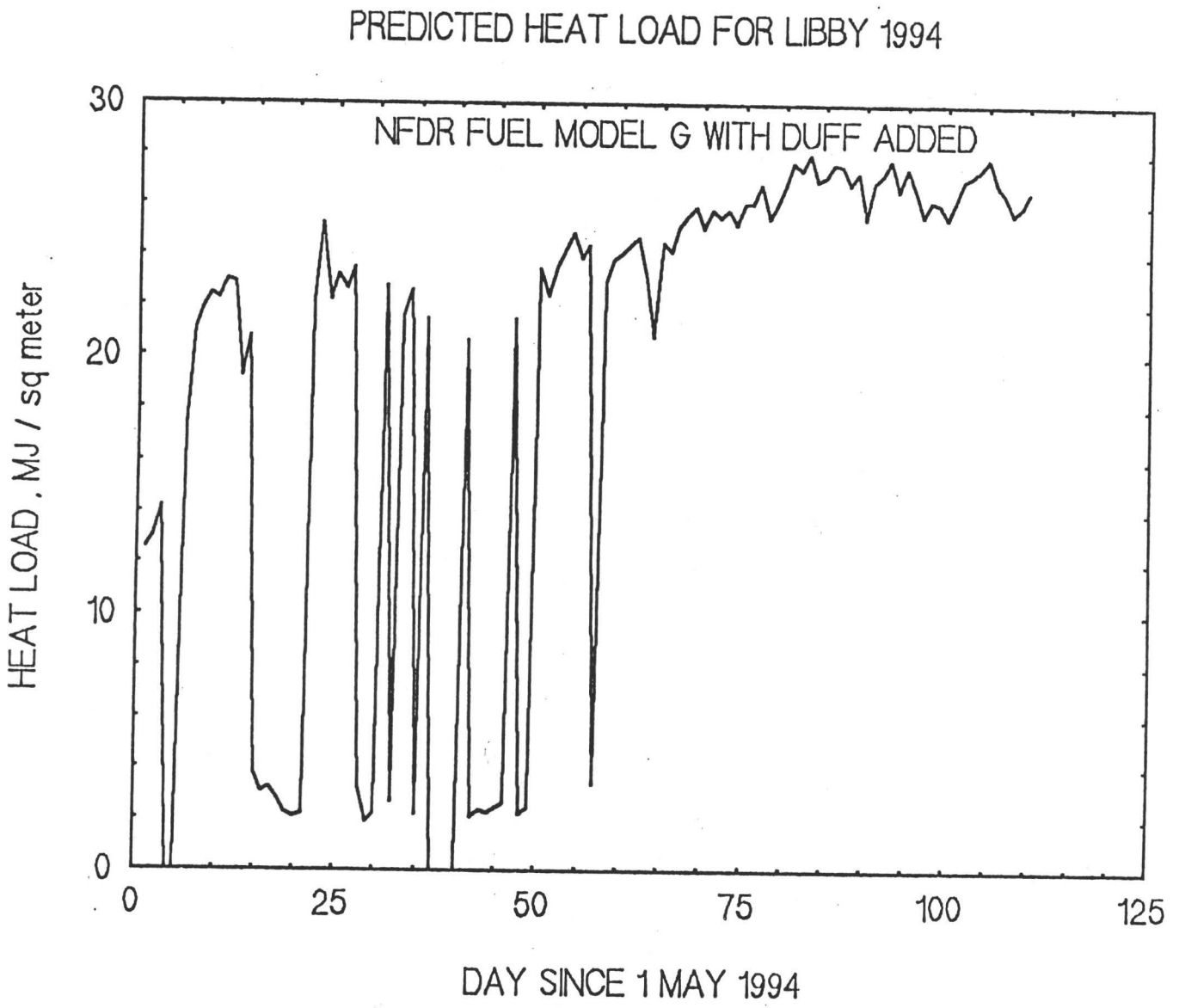

Fig. 4 Seasonal variation at Libby, Montana for early part of 1994 fire season of simulated heat load, including duff burning, for nine minutes following ignition of large surface fuels.

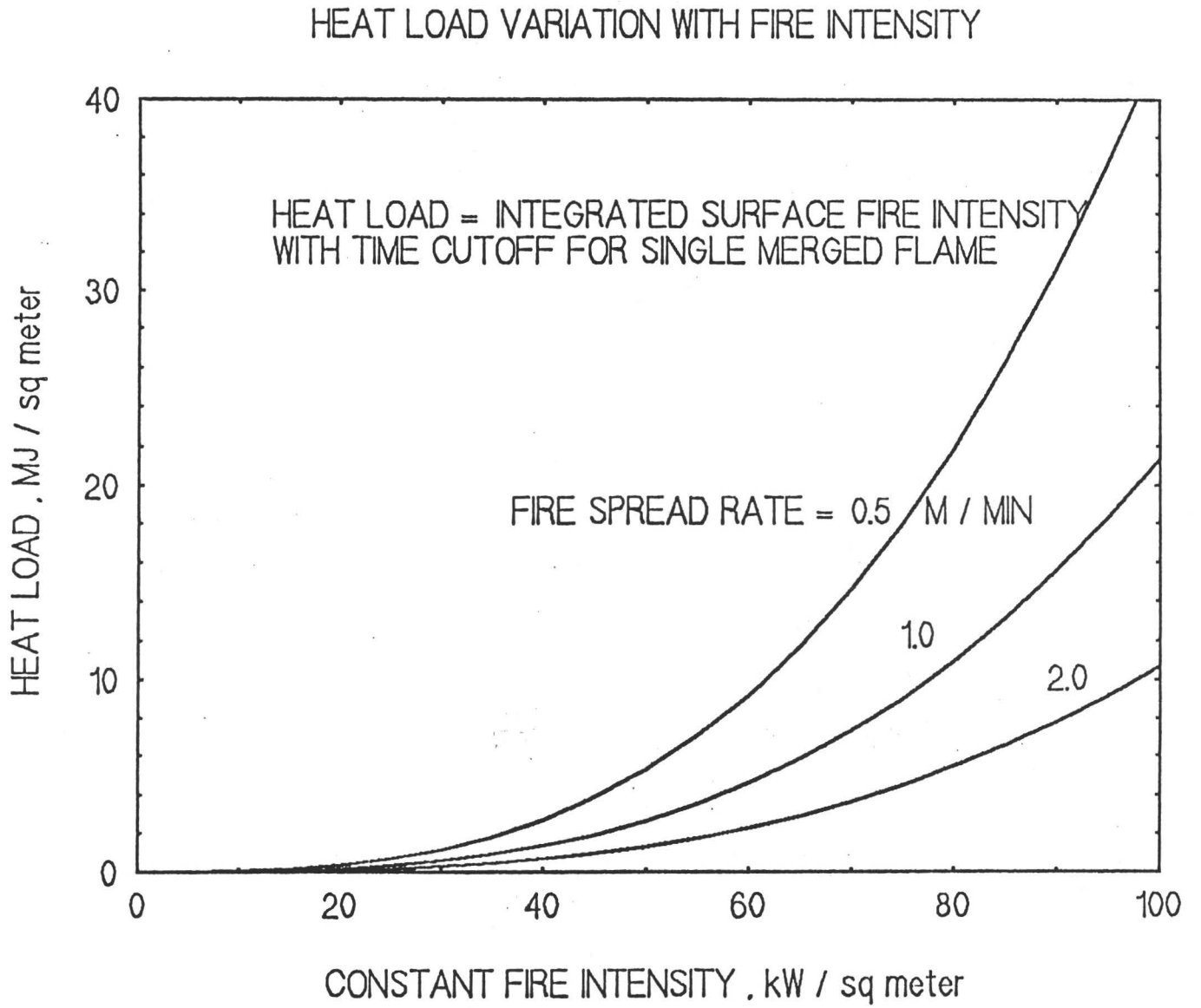

Fig. 5 Variation of heat load with fire intensity and spread rate, under the assumption that the fire creates a single flame structure with base dimension equal to the spread rate times the duration of the averaging time for intensity.

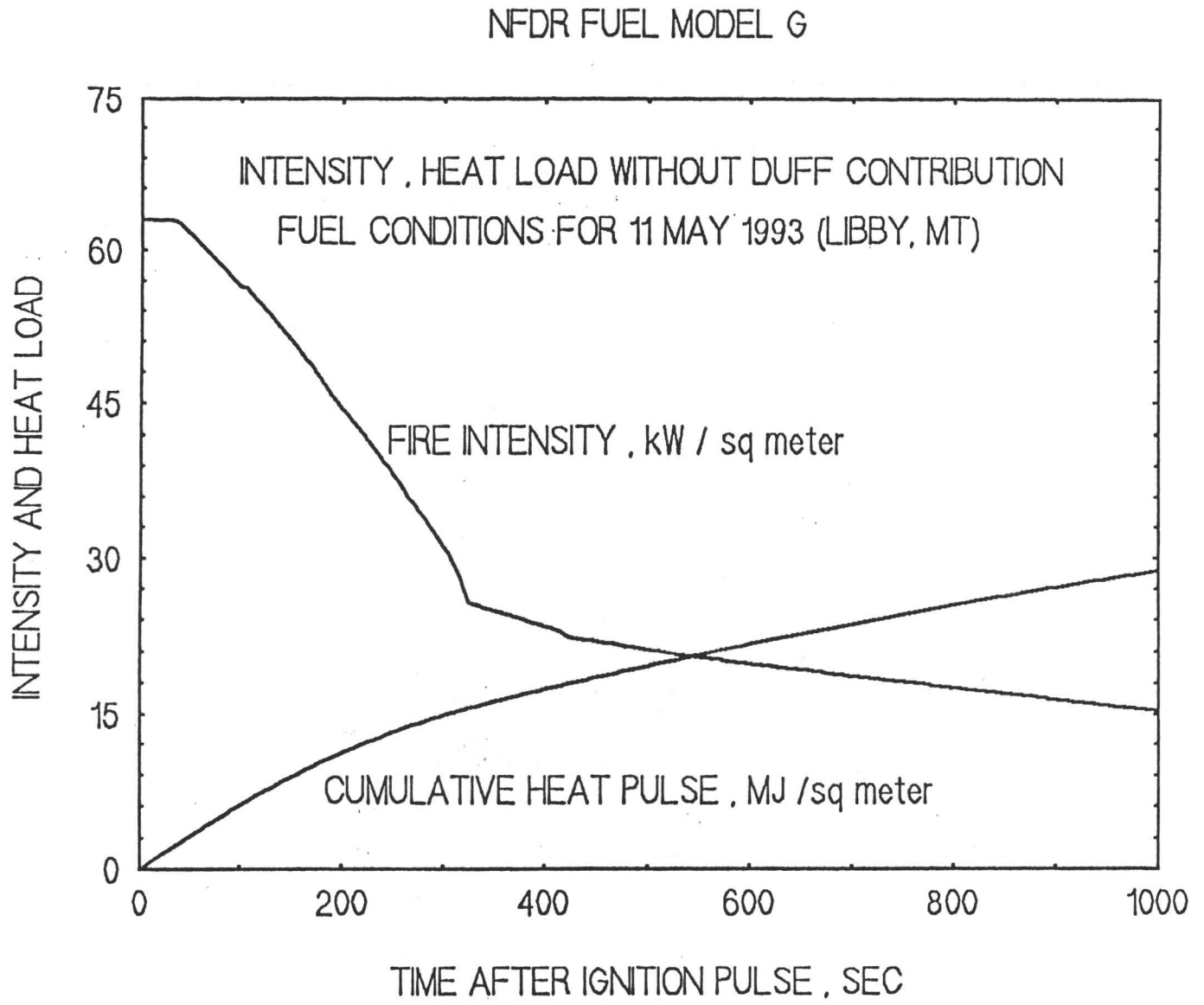

Fig. 6 Post-ignition fire intensity history and cumulative heat pulse for burning of surface fuels under conditions of 11 May 1993 at Libby, Montana.

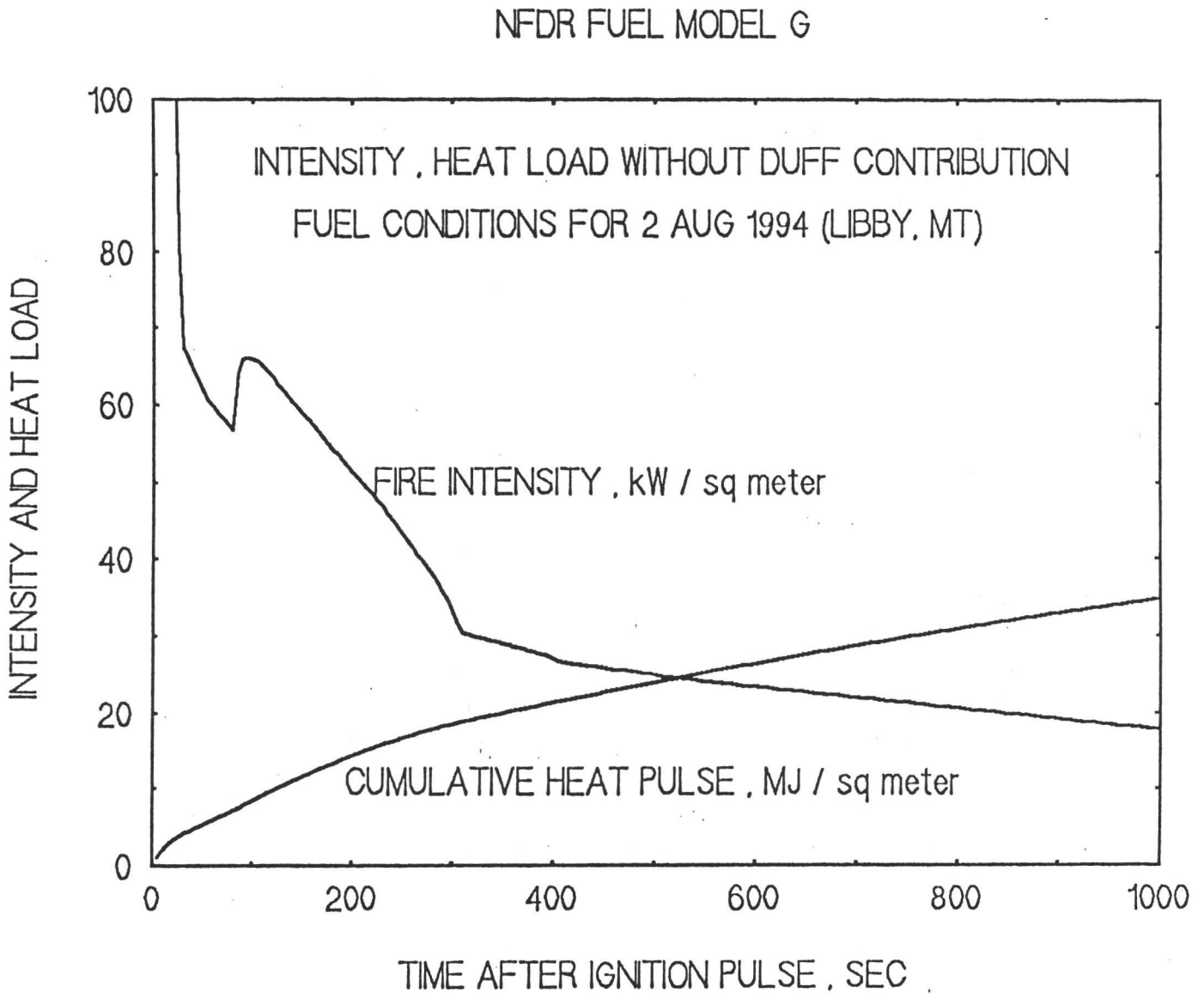

Fig. 7 Post-ignition fire intensity history and cumulative heat pulse for burning of surface fuels under conditions of 2 Aug 1994 at Libby, Montana.

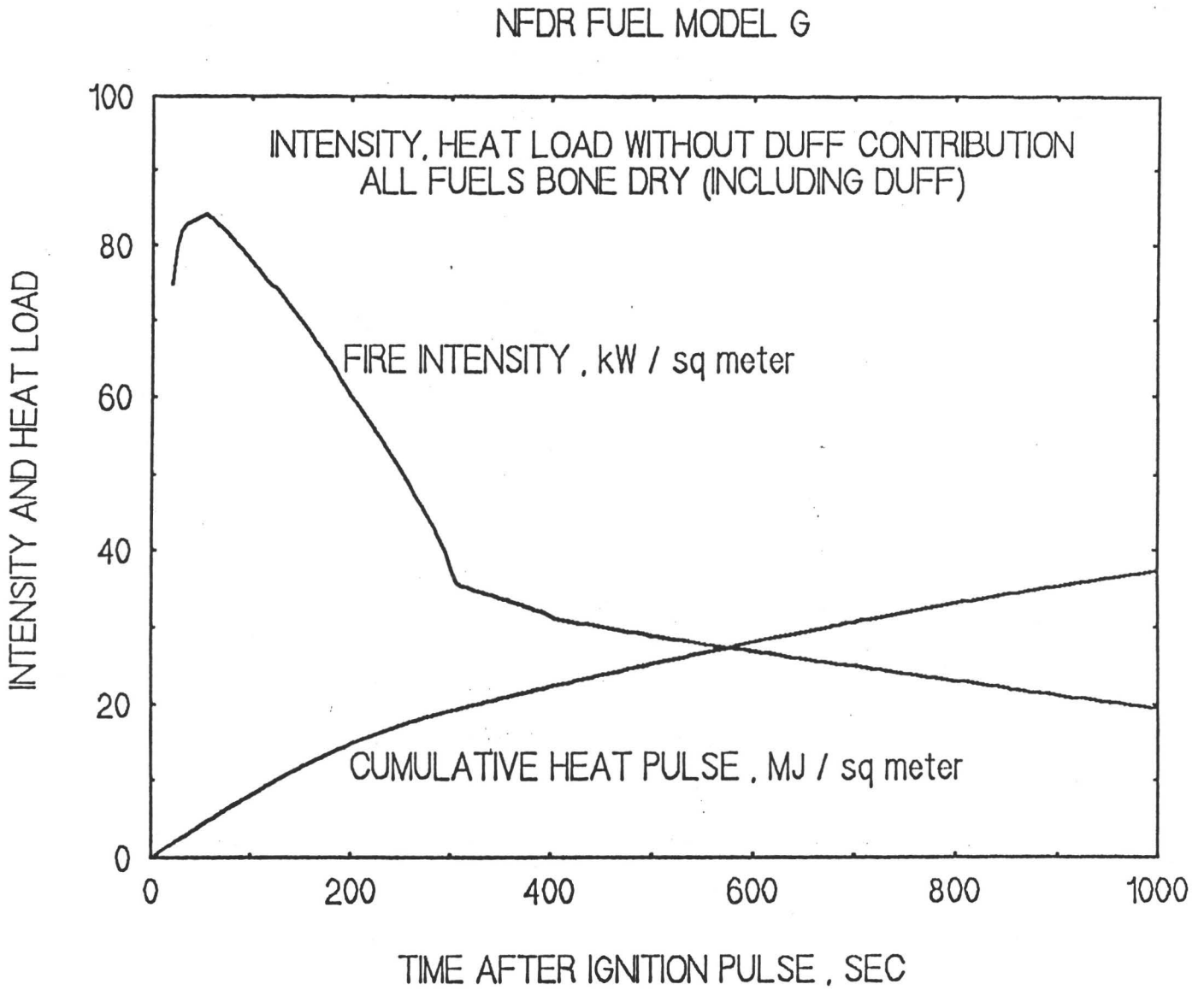

Fig. 8 Post-ignition fire intensity history and cumulative heat pulse for burning of surface fuels under limiting condition that all fuel components, including duff, have no moisture content whatsoever.

APPENDIX A: EQUIVALENT SINGLE SIZE CLASS FUEL BED AND IGNITION PULSE

Purpose

This appendix describes an algorithm that combines loadings of different size classes of fuel, with different intrinsic and extrinsic properties, into a single size class fuel bed description. In generating the single size class equivalent fuel bed, the intention is to preserve many gross features of the original fuel bed -- especially those that influence or control the fire spread rate.

The single size class fuel bed is intended to contain the quantity of fuel that is burned in the leading edge of a spreading fire, producing the same fire edge intensity as the multicomponent fuel bed. While this cannot be mathematically assured, it is assumed that the expression for fractional diameter reduction posited below correctly describes this process. Then the other quantities held constant are consistently transcribed from a multicomponent fuel bed to its single size class equivalent.

The quantities that are maintained invariant in this transcription are:

1) Total fuel surface area per unit volume of fuel bed.

2) Fraction of total fuel bed volume filled with fuel.

3) Mass average values of intrinsic properties of fuels consumed at the fire leading edge.

Nomenclature

Let subscript i designate a fuel component and subscript e the equivalent single component fuel bed quantity. The glossary of fuel and fuel bed descriptors is given below; SI units are used throughout.

W	Ovendry fuel loading, kg / m^2
M	Fuel moisture content, fraction ovendry mass
D	Fuel element diameter (all elements assumed cylindrical), m
σ	Surface area / volume ratio m^{-1}
ρ	Ovendry mass density, kg / m^3
h_c	Specific heat of combustion, ovendry ash-free basis , J / kg
m	Mineral ash content, fraction ovendry ash-free mass
δ	Fractional diameter reduction of fuel element in burning zone at the leading edge of a spreading fire
C	Specific heat capacity , J / kg K

Equivalent Fuel Bed Algorithm

The transcription begins with calculation of the fractional diameter reduction of each fuel component in the burning zone at the leading edge of a spreading fire.

$$\delta_i = \min(a \sigma_i / (\rho_i (1 + b M_i)) , 1)$$

The quantities a and b in this expression are constants to be determined empirically. From thermodynamic considerations, the parameter b should have a numerical value of about 5.0, and this is the value used. For SI units, a value of 3/8 for parameter a corresponds to complete consumption of 0.5 mm diameter foliage with 100% moisture content and of 3.0 mm dia bone dry twigs, if each has an ovendry density of 500 kg / m^3.

Using this quantity, the fraction of the loading of each distinct fuel element enumerated in the multicomponent fuel bed that is consumed in the leading edge of the fire, g_i, is to be found from

$$g_i = 1 - (1 - \delta_i)^2$$

which allows calculation of the ovendry loading of the equivalent fuel bed's single component:

$$W_e = \Sigma \; g_i W_i \; .$$

It is understood that this is the loading of fuel that is promptly burned in the leading edge of the fire in either fuel bed, while in the multicomponent fuel bed the fraction of the loading of each element i that burns is given by g_i. Thus the equivalent loading would have the moisture content M_e, where

$$M_e = \Sigma \; g_i W_i M_i \; / \; W_e \, .$$

To preserve the fractional volume of the fuel bed that is filled with solid fuel, the equivalent particle mass density must be adjusted to:

$$\rho_e = W_e / \Sigma \; (W_i / \rho_i) \, .$$

With the equivalent mass and volume loadings defined, we preserve the fuel surface area per unit volume of fuel bed by selecting the equivalent particle surface / volume ratio according to:

$$\sigma_e = (\rho_e / W_e) / \Sigma \; (W_i / \rho_i) \sigma_i \, .$$

Intrinsic fuel particle properties used in the computation of heat release and in determining the energy required for ignition are then defined in terms of the contributions of the multicomponent fuel bed elements.

$$m_e = \Sigma \; g_i W_i \; m_i \; / W_e$$

$$h_{ce} = \Sigma \; g_i W_i (1 - m_i) \; h_{ci} / (W_e (1 - m_e))$$

$$M_e = \Sigma \; g_i W_i \; M_i \; / W_e$$

$$C_e = \Sigma \; g_i W_i \; C_i \; / W_e \, .$$

Intensity and Burning Time Determination

To establish the intensity and duration of the ignition pulse that would be generated by the burning of the single size class equivalent fuel bed, the burning rate formulation used in the BURNUP model is applied. The diameter reduction rate of a fuel particle exposed to a "fire environment temperature" T_F is given by Albini and Reinhardt [1995]:

$$dD/dt = - h_{eff} ((T_F - T_c) / 255) (446 / \rho_e) / (a' + b' M_e), \quad m/s$$

where

h_{eff} is the effective film heat transfer coefficient including radiant heat transfer, $W / m^2 K$

T_F is the "fire environment temperature", a function of the fire intensity,

T_c is the temperature of the pyrolyzing solid fuel element, here set to 673 K (400 C)

the density and moisture content of the fuel element are as defined above, and a' and b' are dimensional empirical constants found by Albini and Reinhardt [1995] to be

$$a' = 2.01 \times 10^6 \qquad b' = 3.36 \times 10^6 \qquad J m^3 K .$$

The diameter reduction rate and the initial diameter $(4 / \sigma_e)$ are combined to estimate the duration of the ignition pulse, τ :

$$\tau = (4 / \sigma_e) / dD/dt,$$

which allows estimation of the ignition pulse intensity I* using

$$I^* = W_e h_{ce} / \tau .$$

The set of equations is closed using the relationship between fire environment temperature and fire intensity incorporated in the BURNUP model by the function TEMPF:

$$T_F = \text{TEMPF}(I^* , r , T_a),$$

where T_a is the ambient temperature (available from fire danger rating archival data) and the "mixing parameter" r is arbitrarily fixed at 2.03, a value midway between minimum and maximum values found [Albini et al 1995] to fit experimental laboratory crib burn data best. This function is graphed in figure A1 for 300 K ambient temperature. Note that there is a maximum fire environment temperature; for extreme fire intensity, the TEMPF function reduces to the product

$$\lim_{I^* \to \infty} (\text{TEMPF}(I^* , r , T_a)) = (1 + r) T_a$$

These equations can solved by binary search, starting with limits of fire intensity set by $I^* = 0$ and $I^* = I^*_{max}$ and halving the interval on each iteration. I^*_{max} is found by using the maximum of T_F in the expression for d D / d t.

Concluding observations

While the intensity and time values resulting from this algorithm are internally consistent and represent a reasonable approximation to what one might anticipate to result from the multicomponent fuel bed as a spreading fire intensity pulse, it suffers from the following serious defects:

1) The ignition intensity and duration are independent of the powerful influences of wind and slope;

2) The influence of the arrangement of the components (compactness or void volume fraction) is nil, and

3) The algorithm yields substantial fire intensities under conditions of fuel moisture that are too great to permit a surface fire to spread.

Attempts were made to reconcile this method of deriving an ignition pulse with the moisture limit on surface fire spread using the empirically determined moisture of extinction for the fuel model. The intensity found from the expression above for I* was multiplied by a monotonically decreasing function of the ratio (M_e / M_{ext}) where M_{ext} is the fuel model's moisture of extinction. Several functional forms were tried, and each "worked" in the sense that the modified algorithm would yield either zero intensity or a very low intensity (depending on the specific functional form chosen) when the single component fuel bed moisture content approached the moisture of extinction. This would in turn result in no ignition of larger fuel components when the moisture contents of the smaller fuel components was high enough. With such a modification, deficiency number 3 is alleviated, but the other two remain.

These remaining defects are arguably unimportant in assessing the potential heat load of the larger and slower drying surface fuels and duff. But it is difficult logically to reconcile toleration of this lack of realism with any effort to achieve a more realistic ignition pulse. If a realistic ignition pulse is desirable, then perhaps it would be best to turn to the model for the spreading surface fire and extract an ignition pulse prediction from it. Using the algorithm outlined above seems only to complicate the creation of the heat load index, not to make it more realistic.

FIGURE DESCRIPTION

Fig. A1 Fire environment temperature function used to estimate igniting fire intensity.

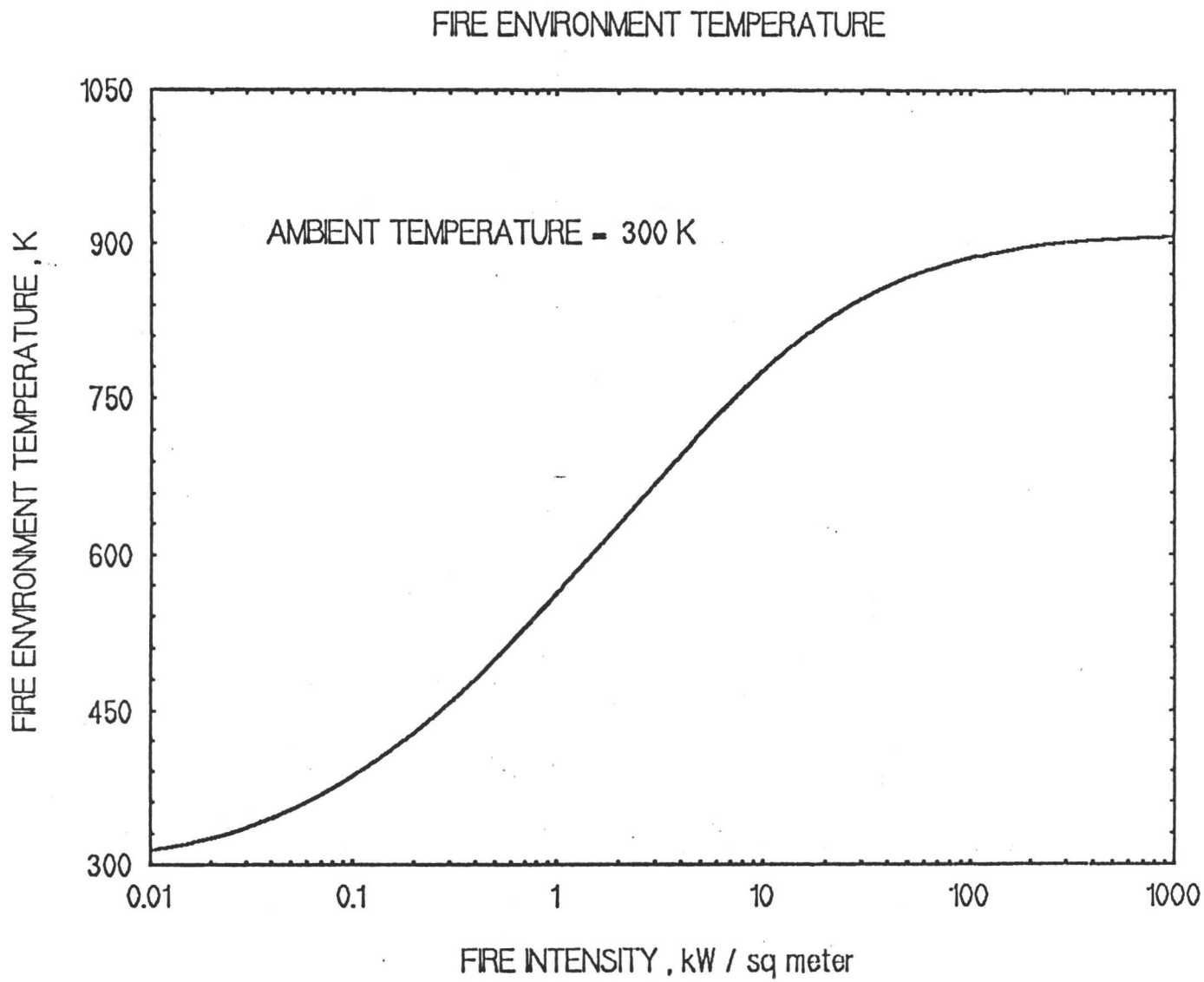

Fig. A1 Fire environment temperature function used to estimate igniting fire intensity.

APPENDIX B: FIRE INTENSITY AND HEAT PULSE DETERMINATION

Purpose

To derive a numerical quantity representative of the intensity and energy output of the enduring fire that burns in large woody fuels and duff once ignited by a spreading surface fire, the BURNUP computer model is used to simulate this fire's intensity history. The intent is to integrate this intensity history over an appropriate period of time following the passage of the igniting fire for the purpose of deriving a measure of the energy release per unit of burned area. The problem arises that the largest surface fuels and the duff can continue to burn for hours after the passage of the fire front, and the behavior of this phase of the fire is not that of immediate concern here. Thus the time integral of the intensity history must be truncated to prevent the resulting heat load quantity from being overly sensitive to this long duration, low intensity, spatially isolated burning. The challenge is to choose a relevant time period over which to cumulate the fire intensity.

Integration time algorithm

It is well known to experienced fire behavior observors that a large area burning simultaneously (such as a broadcast burn of harvest debris) will not sustain a single large flame structure unless the intensity of burning is large enough. If the average area intensity (kW / m^2) is too small or the size of the burning area is too large, the fire will break up into some number of smaller areas that each contribute to a common flame structure but that appear to burn essentially independently. This phenomenology has been investigated experimentally under laboratory conditions in a scaled mass fire experiment [Heskestad 1991], with the result that the characteristic base dimension (D) of the individual common-flame fires is related to the area-average intensity I* by:

$$I^* = G\, D^{1/2} \;\; ; \;\; G = 53 \;\; kW / m^{5/2}$$

One of the intended uses of the heat load index being explored here is to characterize the heat load contribution to the assessment of the fire's resistance to control, as in the "fire characteristics chart" introduced by Andrews and Rothermel [1982]. Because of this intended use it seemed a reasonable choice to use the integration time that would characterize the largest single flame structure that would be observed in a large free-burning fire in the fuel community of interest. To this end, it was posited that the characteristic base dimension of interest would have to be roughly the distance traveled by the head of the spreading fire during the intensity integration period. So if the head fire spread rate is R and the integration time to be determined is τ, then

$$R\,\tau = D$$

and

$$I^* = \int_0^{\tau} I(t')\, dt' \;\; / \;\; \tau \; .$$

Considered as a function of the integration time τ the average intensity I* may initially rise, but ultimately will become monotone decreasing. So long as I* exceeds the limiting value given by Heskestad's empirical relationship, a common flame structure of base dimension D could be maintained. But when I* falls below this value, this determines the largest single flame structure that could be expected from this model. (The model implicitly equates lateral and longitudinal dimensions of the flame structure emerging behind a wide linear fire front, which seems a

asonable postulate, but an untested one.) These equations were coded into an algorithm that returns the heat load ($I^* \tau$) when supplied with the fire intensity history $I(t')$ and the spread rate R.

Figure B1 shows how the heat load varies with the fire intensity and spread rate in the (unrealistic) case of constant fire intensity. If $I(t')$ is constant with t' ($= I$), then it is readily derived that

$$I^* \tau = I^3 / (G^2 R),$$

which is the equation graphed.

Duff burning contribution

The intensity I^* above refers to the intensity of the fire in surface fuels, of course. The burning of duff, if any is present, not only contributes to the burning of some surface fuels, but adds to the heat load on the site. The model for duff burning is based on the laboratory findings of Frandsen [1991a] for the rate of burning of moist peat and the heat evolved from its burning [1991b], and on an empirical correlation of the fraction of the duff loading present that is ultimately consumed by burning once ignited [Brown, Marsden, Ryan, and Reinhardt 1985] with the average moisture content of the duff. These three relationships permit the straightforward derivation of equations for the intensity contribution of the burning duff (I_d) and the duration of the duff burning (t_d).

Let W_d be the ovendry duff loading and M_d the average duff moisture content. The product of the heat evolved per unit mass of peat burned (15×10^3 kJ / kg) and the rate of its burning (kg / m^2 s) gives the duff burning intensity from Frandsen's findings:

$$I_d = \max(11.25 - 4.05 M_d , 0) , \text{ kW} / \text{m}^2$$

The fraction (f_d) of the duff loading present that is predicted to burn is, from Brown et al:

$$f_d = \max(0.837 - 0.426 M_d , 0)$$

Combining these relationships and using the duff loading gives the duff burning time:

$$t_d = 15 \times 10^3 f_d W_d / I_d , \text{ s} .$$

Note that the limiting duff moisture content arises from the expression for f_d , so if M_d equals or exceeds 1.96, it is predicted that no duff burns, even though Frandsen's formula would predict 3.29 kW / m^2 . Thus the duff intensity contribution is limited to this minimum value and the maximum of 11.25 kW / m^2 .

REFERENCES

Albini, F. A. 1994a: Program BURNUP, a simulation model of the burning of large woody natural fuels. Final report on Research Grant INT-92754-GR USDA Forest Service, Intermountain Research Station to Montana State University Mechanical Engineering Department. On file at Intermountain Fire Sciences Laboratory, Missoula MT.

Albini, F. A. 1994b: Memorandum report Re: Green Plan Research Grant "A physical model for crown fire behavior" to Brian J. Stocks, Forestry Canada Ontario Region, Great Lakes Forestry Research Centre 17 Oct 1994.

Albini, F. A., and E. D. Reinhardt, 1995: Modeling ignition and burning rate of large woody natural fuels. International Journal of Wildland Fire (in press).

Albini, F. A., J. K. Brown, E. D. Reinhardt, and R. D. Ottmar, 1995: Calibration of a large fuel burnout model. Submitted International Journal of Wildland Fire.

Andrews, P. L., and R. C. Rothermel, 1982: Charts for interpreting wildland fire behavior characteristics. USDA Forest Service General Technical Report INT-131, Intermountain Research Station, Ogden UT, 21 pp.

Brown, J. K., M. A. Marsden, K. C. Ryan, and E. D. Reinhardt, 1985: Predicting duff and woody fuel consumption in the northern rocky mountains. USDA Forest Service Research Paper INT-237, Intermountain Research Station, Ogden UT. 23 pp.

Burgan, R. E., J. D. Cohen, and J. E. Deeming, 1977: Manually calculating fire-danger ratings -- 1978 National Fire Danger Rating System. USDA For. Serv. Gen. Tech. Rep. INT-40, Intermountain Resch. Station Ogden UT.

Canadian Forestry Service Fire Danger Working Group, 1987: Canadian Forest Fire Danger Rating System -- Users' Guide. Canadian Forestry Service unnumbered publication as 3-ring binder.

Frandsen, W. H., 1991a: Burning rate of smoldering peat. Northwest Science, Vol 65 No 4 pp 166-172.

Frandsen, W. H., 1991b: Heat evolved from smoldering peat. International Journal of Wildland Fire Vol 1 No 3 pp 197-204.

Heskestad, G., 1991: A reduced-scale mass fire experiment. Combustion and Flame, Vol 83, pp 293-301.

NOT FOR DISTRIBUTION

CALIBRATION OF A LARGE FUEL BURNOUT MODEL

Frank A. Albini*, James K. Brown**,
Elizabeth D. Reinhardt+, and Roger D. Ottmar++

December 1994
Revised April 1995

* Adjunct Professor
Mechanical Engineering Department — Telephone (406)994-6298
Montana State University — FAX (406)994-6292
Bozeman MT 59717 — umefa@msu.oscs.Montana.edu

** Project Leader, USDA Forest Service
Intermountain Fire Sciences Laboratory — Telephone (406)329-4803
P. O. Box 8089 — FAX (406)329-4877
Missoula MT 59807 — fswa/s=J.Brown/ou1=s22L01A@mhs.attmail.com

+ Research Forester, USDA Forest Service
Intermountain Fire Sciences Laboratory — Telephone (406)329-4836
P. O. Box 8089 — FAX (406)329-4877
Missoula MT 59807 — fswa/s=E.Reinhardt/ou1=s22L01A@mhs.attmail.com

++ Project Leader, USDA Forest Service
Forestry Sciences Laboratory — Telephone (206)553-7815
4043 Roosevelt Way, NE — FAX (206)553-2039
Seattle WA 98105 — fswa/s=R.Ottmar/ou1=r06F05A@mhs.attmail.com

Key words: Fuel reduction, heat release, intensity, burning rate

ABSTRACT

A computer simulation of the burning of large woody natural fuels has been created. The model simulates flaming combustion of large woody surface fuels but includes the influence of smoldering duff on this burning. This paper describes calibration of empirical constants in the model using data from laboratory crib burns and from prescribed burns in harvest debris and in natural fuel accumulations. The calibrated model reproduced laboratory crib burning rates and natural fuel loading reductions with acceptable accuracy.

INTRODUCTION

It has long been recognized that the process of fire spread in wildland fuels is largely controlled by those fuel components with the largest surface/volume ratios [Brown and Davis 1973, Luke and MacArthur 1977, Chandler et al 1983]. Because of the dominant importance of the finest fuels in controlling spread rate, modelers of wildland fire behavior have focused on these components almost exclusively [Rothermel 1972, Grishin 1981, 1992, Albini 1986]. But in assessing the effects of a wildland fire it is often more important to be able to predict the amount of duff consumed or the rate and amount of consumption of large woody fuels than to predict the speed with which an igniting surface fire would propagate over the burn site.

Most studies of the quantity of consumption of duff and of large woody fuels have been empirical in nature [see recent summary in Brown, Reinhardt and Fischer 1991] and serve well the purpose of predicting fuel quantity reduction. But occasions arise when one desires to predict the rate of heat release from burning of large woody fuels. Such predictions might be used for estimating the rate of heat transfer to the soil [Hungerford 1990] or the maximum distance of potential spot fires [Albini 1981]. In this case one must turn either to correlations of the burning rates of compartments and wood cribs [Harmathy 1972ab, Drysdale 1985, Anderson 1990] or to a suspect model for the burnout of natural fuels based mostly on conjecture [Albini 1976].

Collaborative research addressing this deficiency is currently under way, involving USDA Forest Service personnel at the Intermountain Fire Sciences Laboratory in Missoula, Montana and the Mechanical Engineering Department at Montana State University in Bozeman, Montana. The objective of this research is creation of a model for the rate of

burning of large woody natural fuels based more firmly upon physical process models and making use of field burn data from several sources to calibrate empirical factors. This paper reports calibration of empirical constants used in the model to control the rate of fuel burning and the quantity of large woody surface fuel consumed. The roles of the empirical parameters are explained more fully in the overviews of process simulation and model structure below.

OVERVIEW OF PROCESS SIMULATION

The simulation that has been constructed attempts to approximate the physical processes involved in the burning of large woody natural fuels not with the precision that would be needed in the simulation of an industrial combustion process, but with enough realism to assure sensitivity of model predictions to parameters widely recognized to be important.

For example, the burning rate of any given fuel element is greater when it is thrust into a fiercely burning furnace than when it is simply kindled with a few smaller burning elements. And in either environment its burning rate decreases as its moisture content increases. These sensitivities are assured by modeling the rate of burning of a fuel element as being proportional to the rate at which heat is transferred to the element and inversely proportional to the heat required to raise a unit volume of it to the temperature at which it is converted to char. This crude approximation of the solid fuel combustion process is used in the model discussed here.

The simplest model for the rate of heat transfer to a fuel element from its environment, known as a Newtonian film heat transfer model [Incropera and DeWitt 1985], is that the

rate is proportional to the difference between the temperature of the environment and the temperature of the fuel element's surface. We represent the heating environment experienced by a fuel element in terms of a "fire environment temperature". This term represents the equilibrium temperature that would be achieved by an inert object of roughly the same size and surface character as the fuel element if it were to reside for a long enough time in an unchanging environment the same as that being experienced by the fuel element at the instant considered. The representation of this quantity in terms of the local rate of heat release per unit ground area (*i.e.* the local fire intensity) and the proximity of burning neighbor elements involves empirical parameters whose values influence the prediction of burning rate.

Mathematical completeness, or "closure", of the model is achieved by summing up the rates at which all the fuel elements are burning to obtain the total rate of heat release per unit area of the burn site. In forming this sum, we examine each fuel size class in terms of the degree to which it interacts with other fuel elements of the same size and smaller.

This is done to allow accomodation of the fact that, at any moment, some small size classes may have been completely burned up, larger ones may be burning, and even larger ones may not yet be ignited. In such a situation, some components of a given size class will be experiencing a fire intensity that is more or less than the site-average fire intensity, and this variation can be accounted for.

Description of the interaction of fuel elements involves an empirical parameter whose value selection is described below. Note that it is necessary to consider only "the same and smaller sizes" to avoid double counting of fuel size classes. The model uses the oversimplification that the burning rate of a given size class is influenced by the burning of

size classes larger than its own only through the contribution of the larger elements to the site-average fire intensity. Fuel elements that do not interact with any other surface fuel elements are assumed to be exposed to or resting upon the surface of the burn site, so experience a fire intensity given by the sum of the site-average fire intensity due to the burning of all surface fuels plus the intensity contributed by the burning of duff, if any.

The following sections give technical details of inputs to the model, describe more explicitly the mathematical algorithms, and identify the empirical parameters whose values are determined by matching model predictions to data. Those not interested in such details may wish to skip to the sections on calibration and testing.

OVERVIEW OF MODEL STRUCTURE

The model exists in the form of a set of computer algorithms implementing a time-based simulation with multiple event-based branches. The code runs on a personal computer in an interactive mode, with user input prompted and menu aided. The algorithms are conceptually simple and their operations can be broadly outlined briefly [Albini 1994] but a detailed description of the sequence of steps in some parts of the model devolves to a reading of the FORTRAN source code. We strive here for a balance between thoroughness and tedium.

Input to the model is a complete description of the fuel on the burn site, some parameters that control the operation and performance of the model, and some environmental variables that are necessary for completeness but are not important in determining the model predictions. To facilitate repeated model exercises, data files can be archived and retrieved

as fuel description packages and as environmental and program-control packages. SI (metric) units are used for both input and output.

Each surface fuel category is described by a unique alphanumeric name, its loading (dry mass per unit area, kg/m^2), surface/volume ratio, m^{-1}, and moisture mass fraction, as well as some thermophysical properties, assessed in ovendry condition: heat of combustion, J/kg, ash fraction, mass density, kg/m^3, specific heat capacity, J/kg K, and thermal conductivity, W/m K. For each category also must be specified an ignition temperature and a "pyrolysis temperature" (a hypothetical temperature at which solid fuel is converted to char and gaseous pyrolyzate) which is used to approximate the pyrolysis process as simple sublimation.

Other data required are the intensity (power per unit area, kW/m^2) and residence time, s, of an igniting heat pulse, windspeed, m/s, at the top of the fuel bed, depth of the fuel bed, m, ambient temperature, ^oC, duff loading (dry mass per unit area, kg/m^2) and duff moisture fraction, time step size, s, and number of time steps to be simulated, and three dimensionless empirical parameters whose numerical values are the subject of this investigation.

It should be noted that inclusion of windspeed and fuel bed depth as input quantities may be misleading. The speed of the flow of flame gases across the cylindrical fuel elements is derived as the vector sum of the windspeed, assumed horizontal, and the buoyancy induced vertical speed at the top of the fuel bed. This representative speed is used in determining the rate of heat transfer from flame gas to fuel by forced convection. The far more important and direct influence of wind on the rate of burning of duff and surface fuels is not modeled. Implicitly, calm conditions are presumed to exist and model sensitivity to windspeed is minimal.

Once the data described above are input, the surface fuel categories are sorted in order of increasing size, moisture content, and density. Then the loading of each category is parsed into components that are deemed to be interacting with other categories in its own size class and smaller ones, and with no other surface fuel elements. Note that the number of components in each category is the number of "smaller" size categories than itself plus two. The parsing depends upon the value of a parameter that is proportional to the product of the volume per unit area of the smaller category and the surface/volume ratio of the larger category whose loading is being parsed. The constant of proportionality is one of the empirical constants whose value is to be fixed (see discussion of fuel category partitioning below).

Once each surface fuel category's loading is thus distributed into interacting pairs, the simulation begins. A steady heat pulse of specified intensity and duration, such as the "reaction intensity" and "residence time" of a surface fire available as output from the BEHAVE system of fire behavior prediction models [Andrews 1986, Andrews and Chase 1989], is applied to the site. From this specified intensity, a fire environment temperature is derived and used to characterize the rate of heat transfer to the surface fuel components. The duff is presumed to commence burning at the end of the igniting heat pulse exposure, if its moisture content is less than about 200%.

The response of each surface fuel component to the igniting heat pulse is calculated in terms of the time required for its elements' outer surfaces to achieve ignition temperature. Sound fuels typically ignite at about 600 K, while rotten fuels may ignite at 550-575 K. Each component whose elements achieve ignition is classified as "lit" and its rate of burning is calculated from the rate of heat transfer to an element of that component and the heat

required to raise an element unit volume to "pyrolysis temperature", including vaporization of its moisture content. If no components are lit during the ignition pulse, the simulation stops with that information displayed.

At the end of the ignition pulse period, the simulation-control clock is set to the duration of the ignition pulse but all event times kept internal to the simulation are reset so that the origin of time for the fuel components corresponds to the instant at which the first surface fuel component ignites. Among other events, the event of burnout of each surface fuel component is forecast and updated during each time step. When the internal clock reaches the time currently forecast for a fuel component to be totally consumed, the component is classified as "out". This means that components of the finest fuel categories may be "out" by the end of the ignition pulse period.

The simulation proceeds by marching time forward. At the beginning of each time step, the diameter reduction rate and dry mass loading reduction rate (burning rate) of each component is available from the previous time step. Also available is the time at which each component ignited (or is predicted to become ignited), at which it burned out (or is predicted to burn out) or at which it stopped burning because its local fire environment temperature fell too low. The model uses these burning rates to compute the rate of heat release per unit area -- fire intensity -- for the burn site as a whole, and the local rate of heat release per unit area for each fuel component. The local intensity is calculated as the sum of the site-average intensity and an incremental intensity computed for each component. The local intensity due to the burning of any given component is computed as the rate of heat release by that component per unit of burn site area *divided by the fraction of the burn site area occupied by that component.* Subtracting from this quantity the rate of heat release per unit of burn site area for the component, to avoid double counting, yields the

incremental local intensity for that component. When this incremental local intensity is added to the site-average intensity, the result represents the local fire intensity that would be experienced by the interaction partner of that burning component.

For each time step, the model examines each surface fuel category, component-by-component. Based on the fraction of each category's loading that is currently burning, a "mixing parameter" is calculated and used, along with the local fire intensity, to compute a local fire environment temperature. Two empirical constants are used in computing the mixing parameter (see "fire environment temperature" discussion below). The best choice of values for these parameters is determined by matching model predictions of laboratory wood crib burning rates to experimental data, as described below.

The fraction of each surface fuel category loading that does not interact with any other surface fuel element is assumed to interact with duff. The rate of duff burning is modeled as that of smoldering peat [Frandsen 1991a], so is fixed by its moisture content. This burning gives rise to a fire intensity contribution [Frandsen 1991b] that is added to the site-average intensity to determine the fire environment temperature for the affected surface fuel components. Duff burning is presumed to continue until a certain fraction of the total duff loading on site has been consumed. This fraction is computed using an empirical equation that depends only on the average moisture content of the duff layer [Brown *et al* 1985; Brown, Reinhardt, and Fischer 1991]. No attempt is made to modify this fraction to account for possible interaction with burning surface fuels.

The local fire environment temperature is used to calculate the rate of heat transfer to an element of each fuel component to derive its diameter reduction rate and hence its mass loss rate. In the process the projected burnout times are updated as well as the ignition times for

components not yet ignited. By summing over all the burning components, the site-average fire intensity is calculated, along with the incremental fire intensity for each fuel component.

The simulation proceeds until the specified number of time steps have been taken, until all surface fuel components have ceased burning or been consumed, or until the site-average fire intensity due to surface fuel burning falls below a preset minimum value of 0.1 kW/m^2. After the completion of each time step the simulation will, if the user desires, archive the current state of the burn site in terms of the remaining gross and dry total loading and the site-average fire intensity. If desired, this archival output can be expanded to include the dry loading and rate of change of same, diameter and diameter reduction rate, and time of start of surface drying, ignition, and "burnout" for each surface fuel component. At the end of the simulation, a summary of the residual loadings and diameters of each of the surface fuel components can be created. For each entry is also given the initial loading, moisture content, and ignition and burnout times.

In summary, the model simulates the burning process by calculating the rate of heat transfer to an element of each fuel component, based on its environment as characterized by the applicable fire environment temperature. This temperature depends upon the local fire intensity and a "mixing parameter" which in turn depends upon the fractions of each of the interacting fuel categories that are currently burning. From the rate of heat transfer, the diameter reduction rate for each fuel component is calculated, and thus its loading loss rate. The loading loss rate, along with the ash fraction and heat of combustion, gives its contribution to the site average fire intensity as well as to the local intensity, and thus the model is closed.

FIRE ENVIRONMENT TEMPERATURE AND HEAT TRANSFER RATE

As discussed by Albini and Reinhardt [1995], the term "fire environment temperature" represents the temperature of an inert object residing in a steady fire environment that has attained equilibrium between the rates at which heat is transferred to and from the object. In the steady fires created by a propane burner in their laboratory experiments, this temperature was measured using a thermocouple embedded in a cement sphere of sufficient thermal mass that it required two to three minutes to achieve its ultimate steady temperature once placed in the flame. In a field situation, the local fire environment may change so rapidly that such an instrument could not be used successfully. Nevertheless, the concept can profitably be used if the fire environment temperature is understood to be the temperature that such an instrument would achieve in the local fire environment if that environment were to remain unchanged for a time of the order of a minute.

Thus interpreted, this temperature, T_F, can be used to characterize the rate of heat transfer to or from a fuel component exposed to the fire. The net heat transfer rate per unit surface area, q_{net}'', is modeled as the sum of convective and radiative heat transfer rates to a fuel element whose surface temperature is T_S, using an effective film heat transfer coefficient, h_{eff}:

$$q_{net}'' = h_{eff}(T_F - T_S). \qquad (1)$$

This heat transfer rate is averaged over the recent past, up to a specified maximum number of time steps, to obtain a representative value for each fuel component. Using this formulation, the time required for the surface of each fuel element to reach ignition temperature and the rate at which it burns are modeled, using simplified transient temperature response models and energy conservation relationships.

It should be noted here that the maximum number of time steps over which the fuel element heating rate running averages are determined is a parameter that can influence model operation and performance, as is the length of the time step. Model exercises with time steps between 5 and 30 s have been carried out, with little sensitivity noted, but good performance and smoothly varying burning rates seem to be achieved with a time step of about 10 s. The maximum number of time steps over which the heating rate running average is maintained has been fixed at 20 for all the trials done to date. This means that heating rate averaging spans between 100 and 600 s long have been used, with the great majority of exercise done with 200 s running averages. This time span seems appropriate and was selected purposely, and the user is cautioned that large excursions from the tested ranges of these quantities could cause unexpected model behavior.

The burning rate of a fuel element is derived from its rate of diameter reduction. The diameter reduction rate is modeled as the ratio of the current running average heat transfer rate to the heat required to raise a unit volume of the fuel from ambient condition to the pyrolysis temperature (which is also taken to be the fuel element surface temperature while it is burning), including vaporization of the moisture content of the fuel. Heat transfer modeling is described in more detail in Albini and Reinhardt [1995]. For the present purpose we note that the local fire environment temperature is pivotal in establishing the ignition time delay and the rate of burning of fuel components. The sensitivity of this quanitity to empirical constants provides a means of determining the best values for them.

For a fire in natural fuels, we wish to characterize the fire environment for the burn site as a whole, and locally for pairs of interacting fuel elements (the components of each fuel category). In natural fires we are dealing conceptually with rather large actively burning areas. We presume that, for the fire intensity it supports, the area is too large to produce a

single merged flame. Instead, the structure breaks into many distinct smaller flaming areas [Heskestad 1991]. We deal with the whole burning area on an average basis by the artifice of assuming that there is a balance between the site-averaged fire intensity and the average rate at which heat is transferred away from the surface of the fire site.

The flame fluid flow convects heat away from the surface at the rate Q_c'' W/m^2. And heat is radiated away from the surface at the rate Q_r'' W/m^2. We assume both of these rates to be established by the fire environment temperature T_F. The rate of heat transport by upward-flowing hot products of combustion is

$$Q_c'' = \rho U C_p (T_F - T_a), \tag{2}$$

where ρ is the mass density of the fluid, U its mean upward velocity, C_p its specific heat capacity at constant pressure, and T_a is ambient temperature. Note that there is also downward flow of ambient air to replace the fluid flowing upward, but we assume this replacement air to be at temperature T_a and therefore to transport no excess heat. The radiation contribution to the heat loss rate is given by

$$Q_r'' = \varepsilon \sigma (T_F^4 - T_a^4), \tag{3}$$

where ε is the effective area-averaged integrated emissivity referred to the plane at which the temperature T_F is defined, and σ is the Stefan-Boltzmann constant = 5.67 x 10^{-8} W/m^2 K^4. The sum of Q_c'' and Q_r'' should equal the fire intensity, I,

$$Q_c'' + Q_r'' = I. \tag{4}$$

The rate at which solid fuel is turned to gaseous combustion products must be proportional to fire intensity divided by average heat of combustion, so

$$\rho U = (1 + \Phi) I / H_c \tag{5}$$

where Φ is average air/fuel mass ratio and H_c average heat of combustion.

Using equations (2) - (5) to express the relationship between T_F and I gives the form

$$\theta = 1 + r / (1 + A r (\theta + 1)(\theta^2 + 1) / I) \tag{6}$$

where

$$\theta = T_F / T_a , \tag{7}$$

$$A = \varepsilon \sigma T_a^4 , \tag{8}$$

and

$$r = H_c /((1 + \Phi) C_p T_a) \tag{9}$$

is a parameter that depends on the mixture ratio of air to gaseous pyrolyzate. Clearly this number will be small when the area as a whole is characterized, but will be larger if attention is focused on the flame from two fuel elements burning very close to each other. If $\varepsilon = 1$, A is about 0.4 kW/m^2. To account for noncontinuous area coverage by flames and the fact that flame emissivity is less than unity, A is arbitrarily fixed in the model at 0.05 kW/m^2.

Figure 1 shows the modeled variation of T_F with I for a representative range of values of r. The maximum value of r is estimated to be about 2.5 for burning in still air. In the model r is composed of two parts, which are determined empirically. Note that there is a finite maximum temperature for a fire of infinite intensity:

$$\max(T_F) = (1 + r) T_a, \tag{10}$$

so if T_a is 300 K and r is 2.5, the maximum fire environment temperature is 777 C, a value that is representative of flames from intense compartment and crib fires [Hasemi and Tokunaga 1983].

The simulation model uses equation (6) both for site-average fire environment temperature and for a temperature representing the local environment of interacting fuel elements. The values of I and r are adjusted in each case, in order to achieve the following sensitivities:

1) The minimum value of the mixing parameter, r0, is realized when a fuel element is not ignited and does not interact with a burning partner.

2) The maximum value of the mixing parameter, r0 + dr, is realized when a fuel element

is ignited and interacts with a burning partner.

3) An ignited fuel element not interacting with a burning partner should have an intermediate mixing parameter value, r0 + dr/2.

4) Local fire intensity is computed in an expected value sense. Its minimum value is the site-average fire intensity, I_f, to which is added, as appropriate, site-average intensity due to duff burning, I_d, or incremental intensities from burning of the target element and/or its interaction partner.

Table 1 exhibits the rules for computing local fire intensity and mixing parameter values for determining local fire environment temperature. The incremental local fire intensity values are computed from the burning rates for each category, divided by the fraction of the burn site area covered at least once in effective planform area by fuel of the category in question. Estimation of this fraction is based on the following idealization: Each fuel category is assumed to be composed of very many individual elements, each of which has a planform area (length X diameter) that is very small compared to the burn site area over which they are randomly strewn. The fuel element planform area is multiplied by a dimensionless constant K_a and the result is called the "effective planform area", assumed to represent a planform area of influence for each fuel element of the category. Calculation of the area fraction covered and the role of the dimensionless parameter K_a are discussed in the following section.

FUEL ELEMENT INTERACTION PARTITIONING

Partitioning of the loading of each surface fuel category into fractions interacting with other surface fuel categories or with no others is done at the beginning of the simulation and is

not repeated as smaller size components burn out. Because of this aspect of the model, some of the larger sized fuel elements will often be predicted to be burned out more rapidly when they interact with their own size class than when they interact with smaller sizes. This occurs because the smaller sizes burn out, leaving their larger sized interaction partners to burn at reduced local intensities and with smaller mixing parameter values (and hence at lower fire environment temperatures).

The partitioning algorithm proceeds through the list of fuel categories in order of increasing size. In partitioning category i, all size categories from 1 through i are considered. The quantity b_{ij}

$$b_{ij} = K_a \sigma_j w''_i / \rho_i \pi \qquad (11)$$

is computed for each i, j pair using the empirical constant K_a. Here σ_j is the surface area/volume ratio of category j, w''_i the dry loading of category i, and ρ_i the ovendry mass density of fuel category i.

When j is less than i, j represents a smaller size category than does i and b_{ij} can be regarded as the product of the effective planform area per unit area of category i, multiplied by the ratio of the diameters D_i and D_j

$$b_{ij} = (D_i / D_j) b_{ii} \qquad (12)$$

and so b_{ij} can be interpreted heuristically as the maximum fractional diameter reduction of the loading of fuel elements of category i by elements of category j. The parameters b_{ij} are next constrained to be at most unity

$$b_{ij} = \min(1 , b_{ij}) \qquad (13)$$

and the list of fuel components is reexamined for the final partitioning.

For the final partitioning of fuel category i into interaction components, the sum of the

quantities b_{ij} from j = 1 to i is formed. Call this sum B_i. If B_i is less than unity, then the b_{ij} values are taken to be the partition fractions for the loading of category i, and the difference (1 - B_i) is taken to be the fraction of the category not interacting with any other surface fuel. If the sum B_i exceeds unity, then B_i is used to normalize the b_{ij} values which are then used for the partitioning, and the fraction not interacting with any other surface fuel is taken to be zero.

Note that b_{jj} is equal to K_a times the planform area per unit of site area for fuel elements of size j. Recognizing this as the total "effective planform area" of fuel elements of size category j, and assuming the total to be the result of distributing many small contributions, it was shown in Albini [1976] that the expected fraction of the area covered at least once in effective planform area by fuel elements of size class j is approximately β_{jj}, where

$$\beta_{jj} = 1 - \exp(- b_{jj}). \qquad (14)$$

The quantity β_{jj} is used to compute the incremental contribution to the fire intensity due to burning of ignited category j components.

Note the behavior of the partitioning for limiting values of the empirical parameter K_a. If K_a grows large, all the b_{ij} values become unity. In this limit, the partitioning of fuel loadings is uniform over all categories of the same or smaller size and is independent of the empirical parameter. On the other hand, if K_a is small, all the b_{ij} values become small and proportional to K_a. In the limit of vanishingly small K_a, the fuel elements cease to interact. At an intermediate level such that the b_{ij} values are appreciable fractions of unity but do not exceed it, the sum B_i can exceed unity, and the renormalized partitioning can again become largely independent of the value of K_a. The partitioning in this case becomes proportional to the volume per unit area of the various categories.

In the old BURNOUT model [Albini 1976] this partitioning was used, but the b_{ij} values were interpreted, unrealistically, to be proportional to the loading of size category i that was burned out by interaction with category j. This interpretation is logically inconsistent with the assignment of burning times to the categories that can differ by more than an order of magnitude, and it makes predictions of fuel consumption strongly dependent upon the empirical parameter K_a. The present model strives for physical simulation of the fire environment and derives fuel consumption on that basis, so it eliminates the logical inconsistency and lessens model sensitivity to the parameter K_a, but the fuel interaction partitioning algorithm remains somewhat unsatisfying.

BURNING RATE CALIBRATION

As can be seen from the formulations above, no single parameter controls the prediction of the rate of fuel consumption by the model. While it is apparent that increasing r0 and/or dr would lead to prediction of higher fire environment temperatures (see Fig. 1) and hence to more rapid fuel burning, the effect on burning rate of a change in the value of the area factor K_a is not readily apparent. The value of K_a influences the partitioning of the fuel categories into interacting component pairs, but, as described above, the variation of partition fractions is neither monotonic with nor overly sensitive to K_a.

To calibrate the model's prediction of burning rates, we relied upon an extensive set of wood crib burns conducted under controlled conditions at the Intermountain Fire Sciences Laboratory [Anderson 1990]. In these experiments, dimensioned lumber cribs were burned under no-wind conditions while being continuously weighed, and gross weight was recorded as a function of time. Ignition was achieved by including poplar excelsior (long

filaments of wood) in each crib and lighting a small quantity of a liquid hydrocarbon in a pan under the crib. The maximum weight loss rate occurred almost always within the first ten minutes, and this quantity was the focus of the original investigation.

The objective of the set of experiments was to discern the influence of various factors in controlling maximum burning rate, especially the exposed fuel surface area and the vertical vent area of the crib [Harmathy 1972ab, Drysdale 1985]. Therefore some cribs were constructed with the intention of having their burning rates controlled by their vertical vent areas, some were constructed to exhibit burning rates controlled by exposed fuel surface area, and some were constructed with the intention of having the two areas about equally important in controlling the burning rates (see Tables 2, 3). The present model is designed for natural fuel accumulations and so should apply only to the cases where the exposed fuel surface area would control the burning rate. It should predict too high a burning rate when applied to the cribs with vertical vent area control.

We modeled the burning of the cribs using various values for the mixing parameters r0 and dr and using several values of the area factor K_a. For the igniting heat pulse we assumed that the excelsior burned completely in 20 seconds, and used its loading and heat of combustion to derive the intensity of the ignition pulse. Predictions of gross weight as a function of time were compared graphically and subjectively to measured data and a set of parameters was selected that afforded the "best" match to all the data except that from the cribs with burning rates controlled by vertical vent area. In the process of this subjective parameter selection, it was established that the area factor K_a had little influence on predicting the rate of burning, but the parameters r0 and dr were quite influential, as expected.

Figure 2 illustrates the sensitivity of predicted burning rate to the values of r0 and dr for crib HEALP21, one of the moderately loaded (at 300 T/ha!) cribs with burn rate controlled by exposed fuel surface area. The predictions were made using a value of 2.50 for K_a. The values 1.83 and 0.40 were selected for r0 and dr respectively, after examining a very large number of such graphs.

Using these subjectively "best" values for r0 and dr, a series of crib burns were simulated for area factors K_a between 0.05 and 2.5, to explore sensitivity to this factor. Results are shown in Fig. 3 for the lightest (HEA1T014), the heaviest (HEA3T131), and an intermediate weight crib (HEALP21) for the extreme values of K_a used. From these figures it appears that the two values for the area factor give predictions of burning rate about equally satisfactory, but that an intermediate value might do better. These experiments represent exceptionally dry fuels at extremely high loadings. The lightest crib, HEA1T014, has a loading of 190 T/ha; the heaviest, HEA3T131, about 1350 T/ha.

To establish the best value for the area factor K_a, we turn to data on the consumption of natural fuels, as described in the next section. In doing so we are assured that the value of K_a selected will have very little effect on the quality of the predictions of burning rates for the laboratory cribs.

SURFACE FUEL REDUCTION CALIBRATION AND TEST DATA

Keeping the values of r0 and dr fixed, predictions of woody surface fuel loading reductions were made for various values of the area factor K_a, using preburn and postburn fuel inventory data taken during prescribed fire research studies. Predictions were compared to

measured surface fuel reductions, and the value of K_a yielding the best agreement between predictions and measurements was sought. For this purpose, a calibration set of about half the available data was chosen randomly. A value for K_a was chosen to give good agreement between predictions and observations of surface fuel reduction. Then the remaining data were processed in the same fashion and the performance of the model was evaluated against this test set. The data for calibration and test of the model came from three sources:

1) Twenty prescribed burns were carried out in natural fuel accumulations at the University of Montana's Lubrecht Experimental Forest as a doctoral thesis research project [Norum 1975]. These data are identified by the shorthand designation "Lubrecht" below.

2) Thirty six plots in mixed conifer logging slash in northern Idaho were burned over a period of three years for research on fuel reduction by prescribed burning [Reinhardt, Brown, Fischer, and Graham 1991]. These are identified as "Deception Creek" data, for the drainage in which the study was carried out.

3) A series of prescribed burns in logging slash was conducted over a period of several years for various research purposes, by workers at the USDA Forest Service Pacific Northwest Research Station; a broad selection of these burns had data stored in machine-readable format and were made available for use here. These data are identified as "PNW" in what follows.

Each data set includes preburn and postburn inventories of surface fuels and characterization of the duff loading and moisture content. Thermophysical properties (*e.g.*, density, thermal conductivity, specific heat capacity, *etc.*) were not measured, so

representative handbook values were used for these parameters. The character of the igniting fire was not quantified in any of the studies, but it is clear from the fact that a loading reduction was measured for each burn unit that some large surface fuel was ignited and consumed by fire in every case. A set of preliminary model exercises led to the selection of an ignition pulse of 50 kW/m^2 for 60 s (representing the burning of about 0.15 kg/m^2 of kindling fuels) which was sufficient to ignite at least some large surface fuels on all sites.

Nonuniformity of fuel loading can give rise to considerable variation in fuel consumption, especially if ignition effort is concentrated to any degree on fuel accumulations of greater than average loading when burning conditions are marginal. Migration of large fuel elements during burning also takes place. Fuel elements that roll downhill and leave the inventory transect show up as consumed totally by fire, while elements that move onto the transect can appear as an anomolous increase in fuel loading. In this study, surface fuel loading increases in any size class were treated as zero reductions. Such confounding effects are characteristic of field research on wildland fire, and must be accepted as sources of variability.

Each data set has also some unique features which need to be considered in interpreting the calibration and test computations. Some unique aspects of the data sets are outlined and their implications in the present context are discussed below.

Deception Creek

Fuels were the result of recent logging in a decadent stand. Rotten fuels were both preharvest and activity fuels, while sound fuels were mostly activity fuels. Sites were steep,

and fuel loadings were high.

Preburn and postburn fuel loadings were measured on the same twenty permanently marked transects, using the planar intersect technique. Small diameter, 1/4 - 1 (6.35 - 25.4 mm) and 1 - 3 inch (25.4 - 76.2 mm), pieces were counted on six foot (1.83 m) and ten foot (3.05 m) transects, respectively, while larger pieces were recorded by diameter and sound/rotten classification on 50 foot (15.24 m) transects. Unit average preburn and postburn loadings were computed by size class from the transect data, and consumption was computed as the difference between the two. In a few cases, "negative consumption" was computed for one or more size classes, probably as a result of pieces rolling onto the transect, or larger pieces being partially consumed and being counted in a smaller class in the postburn inventory. We assume that this sampling error is small, that pieces rolling onto the line are offset by pieces rolling off, and that the effect of pieces changing size classes disappears when size classes are totaled to estimate total fuel consumption for a unit. For the Deception Creek data, the magnitude of these negative values was small -- an average of 0.8% of preburn loading.

In this study series, 60 logs were more intensively measured on each of 18 units. Moisture content and diameter reduction were measured for each log. The moisture contents were summarized by size class and sound/rotten. These are the moistures used for calibration here. The diameter reduction data showed a lot of variability so we did not use them here.

The Deception Creek data are unusually complete in scope. Surface fuel loadings were inventoried for fuels as small as 1/4 - 1 inch in diameter, and 0 - 1/4 inch loadings were estimated using samples collected from small areas to establish representative relative loadings of 0 - 1/4 and 1/4 - 1 inch components. Fuels were characterized as sound or

rotten and large fuel moisture contents were measured for 18 units. Duff loading and moisture content samples were extensive and the study provided abundant duff reduction measurements from spikes.

The surface fuel consumption data from this set are thorough and thought to be quite reliable. The moisture content range of the larger surface fuels was large, being 32 - 61% (sound) and 50 - 111% (rotten), but most of the fuels under 1 inch (25.4 mm) in diameter were at about 10% moisture content and the litter-derived duff (over the whole study area) was rather shallow and quite dry. Because of these features, the simulation sees each of the sites as readily ignitable, but the range of duff burning influence on surface fuel consumption is rather restricted. Strip headfires up the 50-80% slopes were lit by propane torches to ignite these burns.

The eighteen units with complete fuel moisture data had an average preburn surface fuel loading of 13.9 kg/m^2 and an average surface fuel loading reduction of 6.75 kg/m^2 (49%), with a coefficient of variation of 1/3. The loadings are relatively large for current harvest and utilization practice, but the fractional reduction by burning is not and the unit-to-unit variation is rather small.

Lubrecht

The Lubrecht Experimental Forest burns were carried out in older fuel accumulations under standing timber on slopes varying from steep to nearly flat and, on average, not as steep as at Deception Creek. Fuels included natural fuels and debris from a harvest approximately 50 years earlier.

Woody fuels were inventoried using techniques similar to those applied at Deception Creek. Thirteen sampling planes were used in each unit. Two meter transects were used to tally fuels less than three inches (76.2 mm) in diameter, and four meter transects for larger fuels. As at Deception Creek, preburn and postburn loadings were computed from transect data by size class and consumption was taken to be the difference between the two.

The problem of "negative consumption" was more evident than in the Deception Creek data. In addition to rolling and changing size classes, some Lubrecht transects gained fuels when standing trees fell on them. This did not occur in the Deception Creek data because the burn units were clearcuts or residual trees were very large. Of 20 units burned at Lubrecht, 19 had an increase in loading in at least one size class, and one unit had a total postburn fuel loading greater than the preburn loading.

The biggest contributor to negative fuel consumption appears to be fuels that were tallied as rotten in the preburn inventory and as sound in the postburn inventory. The increases in loading ascribed to the sound classes were treated by our data processing rules as being zero reductions. But the imputed "total consumption" of those rotten components that changed classification is not discernible in the data. The effects of this aberration (which occurred in 13 - 17 of the 20 burns) are that the loading reductions of sound components are understated and those of rotten components overstated. So, if the model worked flawlessly, it would be deemed to have overpredicted consumption of large sound fuels and to have underpredicted large rotten fuel consumption. As "partly rotten" components are not currently modeled, there is no way accurately to account for their effects.

Total surface fuel loadings were relatively light compared to the harvest debris burns, averaging 6.23 kg/m^2 for the 20 units. Large fuel moisture content was not measured for

these burns, but were measured for fuels up to 1 inch in diameter. We used the measured moisture content of the 1/4 - 1 inch fuels for the 1 - 3 inch fuels, and the reported values [Norum 1975, 1976] of the calculated National Fire Danger Rating 1000 hr fuel moisture content for the larger components.

Duff loadings and moisture contents were sampled for each site and the fuel inventory data are considered to be accurately sampled. The burns all seem to have been carried out under moist conditions. In almost every case, the smaller size fuels whose moisture contents were measured had significantly higher moisture contents than were computed for the 1000 hr timelag components. Loadings of 0 - 1/4 inch and 1/4 - 1 inch fuels for these sites were much smaller fractions of the 1 - 3 inch and larger loadings, probably because these were mostly natural fuel accumulations rather than debris from recent harvests. The relatively light loadings of these "kindling" fuels hints that ignition may have occurred nonuniformly on some sites, in local concentrations of surface fuels.

PNW

Data from this extensive set of experimental burns in harvest debris revealed some consistent differences between fuels and burning conditions on the dry interior sites of the Deception Creek and Lubrecht studies and the more moist sites of Western Washington and Oregon. Unlike the Deception Creek and Lubrecht studies, the sites in the PNW study are broadly distributed geographically and in terms of forest type and harvest method. Surface fuel moisture contents were measured. The differences are no doubt real and stem from the soil, climate, and species differences between the two locales.

Preburn fuels were sampled using planar transect methods, with a total transect length of

4000 feet (1.219 km) per site [Sandberg and Ottmar 1983]. Consumption of large woody fuels was estimated not from postburn transects, but from average diameter reductions of a set of 20 - 40 pieces that were banded with wire before and after burning. Moisture content was measured on the pieces that were wired. Quadratic mean diameter was computed for each size class of preburn large fuels based on the transect data, then diameter reduction was applied to this to estimate average postburn diameter. Because of this methodology, "negative consumption" was never observed. The samples to be wired were selected from sound, cured pieces with preburn diameters between three inches (76.2 mm) and 12 inches (304.8 mm).

The physical sizes of the fuel components were larger in the PNW data, but the loadings were not. The mean loading of surface fuels for the PNW burn sites was 7.30 kg/m^2, which is much closer to the Lubrecht natural setting data (6.23 kg/m^2) than to the atypically heavy harvest debris of Deception Creek (13.9 kg/m^2). The duff loadings on the PNW sites were considerably greater than on the Deception Creek sites and less than on the Lubrecht sites, but the PNW duff was typically much more moist than that on either of the interior locale sites. The large sound fuels in the PNW burns were also much more moist than those on either of the other study areas. The combined effects of moist duff and moist large surface fuels led to the smallest mean surface fuel consumption, 3.85 kg/m^2, which is less even than the Lubrecht study average of 4.53 kg/m^2.

The PNW surface fuel consumption data exhibited very little variation from site to site; the standard deviation of surface fuel loading reduction was 1.72 kg/m^2 compared to 2.25 for Deception Creek and 2.46 for Lubrecht. The reason for this consistent difference is not apparent. A contributing factor might be the omission of rotten fuel components from PNW inventories taken before and after each fire, but this was not felt to be a significant

omission since rotten fuels contributed but a small fraction of the surface fuel loadings. But because the variance in surface loading reduction is so small, the influence on loading reduction of various factors thought to be pertinent is difficult to discern and even more difficult to test quantitatively.

MODEL CALIBRATION AND TEST

Eight sites from the Deception Creek data set, ten from Lubrecht, and 15 from PNW were selected randomly for calibration trials. Predictions of surface fuel loading reduction were made for each of the sites, for a range of values of the empirical area factor parameter K_a from 0.6 to 3.0, using an ignition pulse of 50 kW/m^2 for 60 s. This ignition pulse was found by trial and error to be minimally sufficient to ignite at least some large surface fuel on each burn site. The energy density of this ignition pulse is 3 MJ/m^2, which would be released by burning of about 0.15 kg/m^2 of kindling fuel. This quantity of fuel is available on every plot in the data set, as part of the loading of litter and 0 - 1/4 inch diameter surface fuels. Such fuels would be almost completely consumed in about one minute after first ignition at any point, so the modeled ignition pulse is not excessively energetic.

Table 4 shows the results of this calibration trial for each of the three study areas, for Deception Creek and Lubrecht combined, and for all three study areas combined. The Deception Creek and Lubrecht data, considered separately and in combination, are very well predicted by the model, as judged by the fact that the mean square error of prediction is small compared to the variance of the data and that the minimum mean square error occurs near zero mean error of prediction. The PNW data are poorly predicted by the model, with the mean square error of prediction exceeding the variance of the data. In

other words, the model does not predict the variation in the data as well as using a constant prediction equal to the mean of the data.

These observations are quantified by the data presented in Table 5. This table exhibits measures of the degree to which the model predictions fit the data of the calibration set. The quality of this fit can be judged in several ways. If one were dealing with a predictive model that relied upon input data which had no uncertainty (hence, whose predictions were numerically certain) one could simply perform a linear regression of the measured (and therefore somewhat uncertain) surface fuel loading reductions against the model's predictions and use the familiar coefficient of determination (r^2) as a single measure of the fidelity of the model. Additional measures of the quality of the fit of observations to predictions are given in Table 5 in the form of linear functions that would "best" describe scatter plots of the observations against the model predictions.

Fits are of the form $y = a + bx$ and $y = cx$, where x is total surface fuel reduction model prediction and y is measured reduction. Fits are found by determining the values of a and b, or of c, which place the line nearest, in the least mean square sense, to all the point pairs (x,y) in light of the fact that both x and y are subject to errors of measurement. The y values are differences between two experimental measurements, while the x values each depend nonlinearly upon a set of measured quantities. Clearly an "accurate" model would result in a small value (compared to the mean of the observations) for a, and values for b and c near unity. But if such quantities are obtained it does not follow that the model is accurate, but only that its predictions show little bias. It is the variation of these linear fit parameters with the empirical factor K_a, and their consideration in conjunction with the mean and mean square errors of prediction, that yield the modeling insights sought. The interpretation we see in the variation of these fitting parameters with K_a is as follows:

1) The Deception Creek data can be predicted accurately by proper choice of K_a value; strong sensitivity of a and b to choice of K_a and the shallow minimum of mean square error near $K_a = 2.4$ indicates a small number of poorly predicted units, with the predictions being sensitive to the value of K_a.

2) The Lubrecht data are well predicted by the model and the predictions are insensitive to the value of K_a used. There is a trend toward slightly better predictions as K_a increases, continuing even at $K_a = 3$, but there is little improvement to be achieved.

3) The PNW data show a substantial bias that is only weakly sensitive to the value of K_a and this dependence is in the opposite sense to that of the Lubrecht data. This implies that there are some number of units whose fuel reductions are badly overpredicted by the model, that the predictions depend only weakly upon the value of K_a and predictions increase as K_a increases.

Detailed analysis of the individual burn unit results for the various data sets confirms these interpretations. A pleasantly surprising finding from the detailed assessment was that a large majority of the PNW burn units were in fact accurately predicted by the model, but that five were substantially overpredicted. This is visually apparent from a comparison of the scatter plots in Figs. 4 and 5. Fig. 4 is a scatter plot of predicted and measured surface fuel loading reductions from the calibration set of burn units from the Deception Creek and Lubrecht study sites, with the predictions made using $K_a = 2.4$. In Fig. 5, data from 15 PNW sites are added. Note the five units that appear in the lower righthand corner of this plot.

The pattern of these two figures is repeated for the other values of K_a used in the first set of calibration trials. The loading reductions seem to be predicted either very accurately or rather inaccurately. No reason for the inaccurate predictions was apparent in the data, and the predictions are only weakly sensitive to the value of K_a used. But the errors arising from these few burns (15% of the calibration set) forced the calibration of the area factor to the range of quite small values. The second set of calibration trials used a K_a range of 0.10 - 0.50 leading us to the selection of $K_a = 0.4$ as the best compromise value. Clearly a value near 2.4 would better fit the data from Deception Creek and Lubrecht, but a smaller value than 0.10 would be needed to optimize performance against the PNW data, as is apparent from the entries in Table 6.

As with all field data, there are bits of anecdotal information that "explain" some observations. For example, one of the PNW sites for which the model badly overpredicted fuel consumption endured rain for 45 minutes right after ignition. This we discovered while seeking reasons for the large errors of prediction for some sites. But as no search was made to explain very accurate predictions, this discovery is not a research finding but an anecdote.

To minimize one source of misprediction, the duff moisture contents for all units were artificially adjusted to the values that would cause the model to predict the observed duff consumptions. This adjustment reduced the bias (mean error of prediction) by about 1/4 and the rms error of prediction by about 1/3 for the PNW data, but had almost no influence on the prediction errors for the other data, for $K_a = 0.4$. While the adjustment was beneficial where it was expected to have been, it did not dramatically reduce the largest errors. But it is encouraging that the accuracy of predictions improved when a source of error was suppressed.

Figure 6 shows the scatter plot of measurements versus predictions for the calibration data set and Fig. 7 shows the same for the data that were not used in the calibration trials. This scatter plot appears to show better agreement between measurements and predictions than was achieved for the calibration data. This observation is confirmed by the numerical measures of model performance given in Table 6.

Figure 8 is a scatter plot of measurements versus predictions of surface fuel loading reduction for the entire data set, using 0.4 for the value of K_a. Different symbols are used for the data from the three different study areas in Fig. 8, allowing one to discern visually the trends of overprediction for some units of the PNW data set and underprediction of a few units of the Deception Creek data set, with the Lubrecht data clustering near the diagonal line of perfect agreement.

SUMMARY

A simulation model for the burnout of large natural fuels has been assembled and tested. The rate at which fuel elements burn is modeled as a balance between the rate of heat transfer to a burning fuel element and the energy required to heat a unit volume of the fuel to a hypothetical "pyrolysis temperature" at which the fuel sublimes. This artifice permits construction of a relatively simple model for the extraordinarily complex real process of pyrolysis and combustion of the gaseous and solid products.

Heat transfer is calculated as the sum of convective and radiative terms, driven by a "fire

environment temperature" which is modeled as dependent upon the local fire intensity and a pair of empirical parameters that conceptually describe the amount of excess air mingled with combustion products in the flame fluid flow. These parameters control the prediction of burning rate, so numerical values for them were selected by fitting model predictions to measurements of laboratory wood crib burning rates.

The increase in local fire environment temperature when two fuel elements interact was maximal in the laboratory wood cribs, because they were so heavily loaded. For more lightly loaded natural fuel accumulations, the components interact only when they are in close proximity. The probability of such interaction between pairs of fuel components is modeled crudely as being proportional to the fraction of the burn site area that is covered at least once in planform projection by the "effective interaction area" for each pair of fuel components. This area includes an empirical factor that influences the ultimate amount of surface fuel consumption, but only weakly. Prescribed fire studies of surface fuel consumption provided data sufficient to calibrate and test this empirical factor. The numerical value selected for this parameter from this exercise is rather small, and there is evidence that model performance might be further improved by using a smaller value yet, but some ambiguity remains concerning the trend of model performance with this quantity.

The model includes the influence of duff burning on the consumption of surface fuels, by including the contribution of the burning duff to fire intensity for fuel components not interacting with other woody surface fuel. The amount and rate of duff consumption in the model depends upon its moisture content, but the important effect of wind on duff burning rate is omitted. This omission represents a major residual weakness of the model, and it should be used only to represent calm conditions until this deficiency is remedied.

ACKNOWLEDGEMENT

The senior author gratefully acknowledges support of this research by USDA Forest Service, Intermountain Research Station, under research grant INT-92754-GR, and continuing sponsorship and collaboration under research joint venture agreement INT-94947-RJVA. We note with appreciation the special effort by Ms. Roberta Hartford, USDA Forest Service Intermountain Fire Sciences Laboratory, who found, resurrected, and interpreted the laboratory wood crib time series data for us. Critique of an early draft of this paper by Ms. Patricia Andrews, USDA Forest Service Intermountain Fire Sciences Laboratory, Mr. Mark Finney, Systems for Environmental Management, and Dr. Brad Hawkes, Canadian Forestry Service, Pacific Forestry Centre, was generously afforded and proved to be most helpful.

FIGURE DESCRIPTIONS

Fig. 1. Fire environment temperature variation with fire intensity for several values of the "mixing parameter" r (see equations 6-9).

Fig. 2. Predicted burning rates for crib HEALP21 for r0 = 1.8 and three different values of dr, compared to the experimental record of weight as a function of time. By means of many such graphical comparisons, the "best" values of r0 and dr, 1.80 and 0.43 respectively, were selected.

Fig. 3. Weight vs time (solid lines) for a 3.5 kg crib, HEA1T014, a 44 kg crib, HEALP21, and a 200 kg crib, HEA3T131. Model predictions using area factors K_a = 2.50 (long dash) and 0.05 (short dash), and the "best" values for r0 and dr are shown for comparison.

Fig. 4. Scatter plot of calibration exercise predictions and measurements of surface fuel loading reductions for 18 burn sites from data sets for Deception Creek and Lubrecht study areas. Two least squares linear fits are shown; the solid line is constrained to include the origin; the dashed line is not.

Fig. 5. Scatter plot of Fig. 4 with the addition of 15 burn sites from PNW study areas. Note the five severe overpredictions now included.

Fig. 6. Area factor calibration exercise shows acceptable surface fuel reduction predictions using area factor 0.4 and data from all study areas.

Fig. 7. Performance of the model in predicting surface fuel loading reductions for all sites excluded from the calibration exercises.

Fig. 8. Scatter plot superposition of Figs. 6 and 7, using different symbols for the three different study areas. Note underprediction of three Deception Creek units and overprediction of six to eight units from PNW data set.

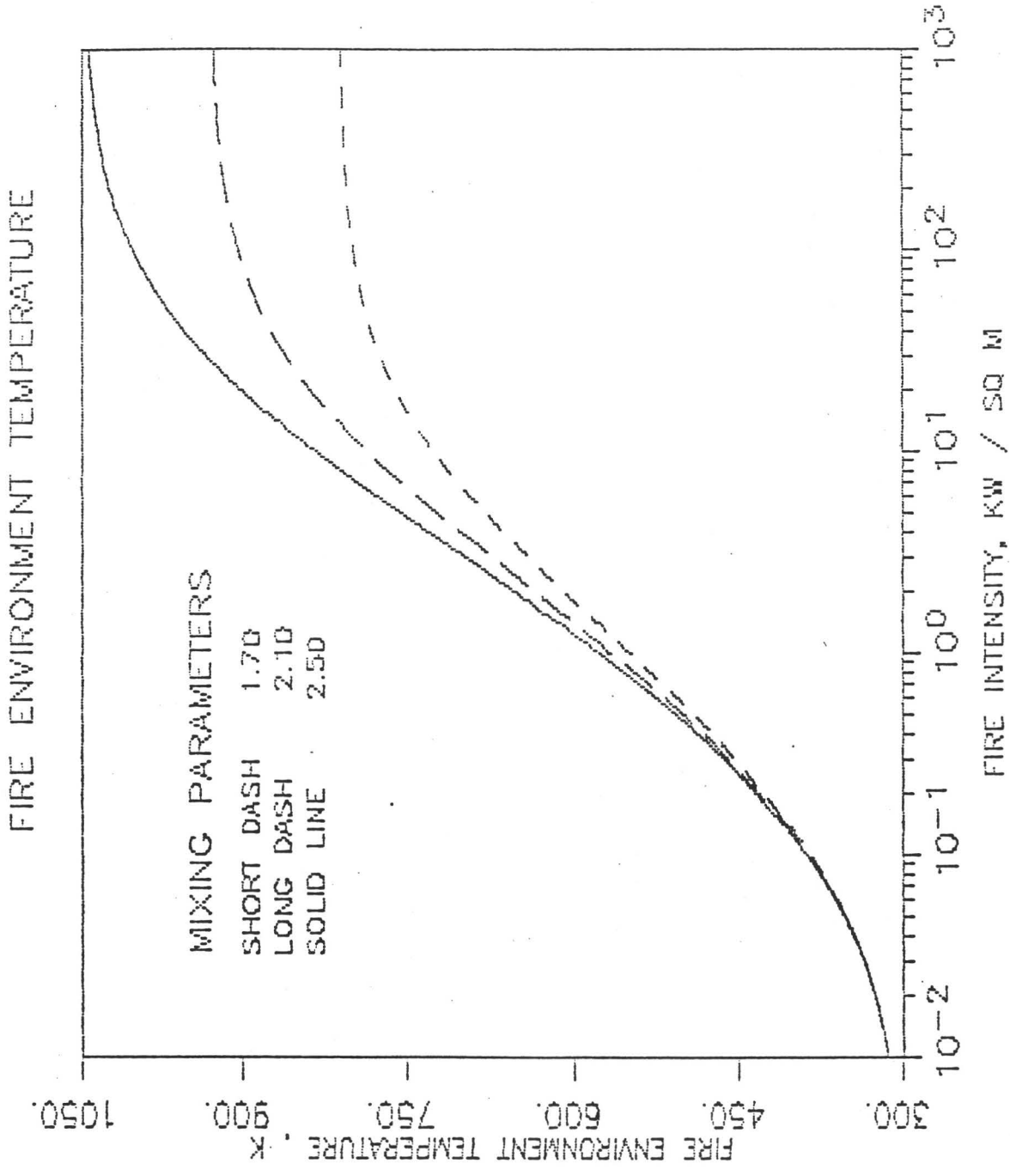

Fig. 1. Fire environment temperature variation with fire intensity for several values of the "mixing parameter" r (see equations 6-9).

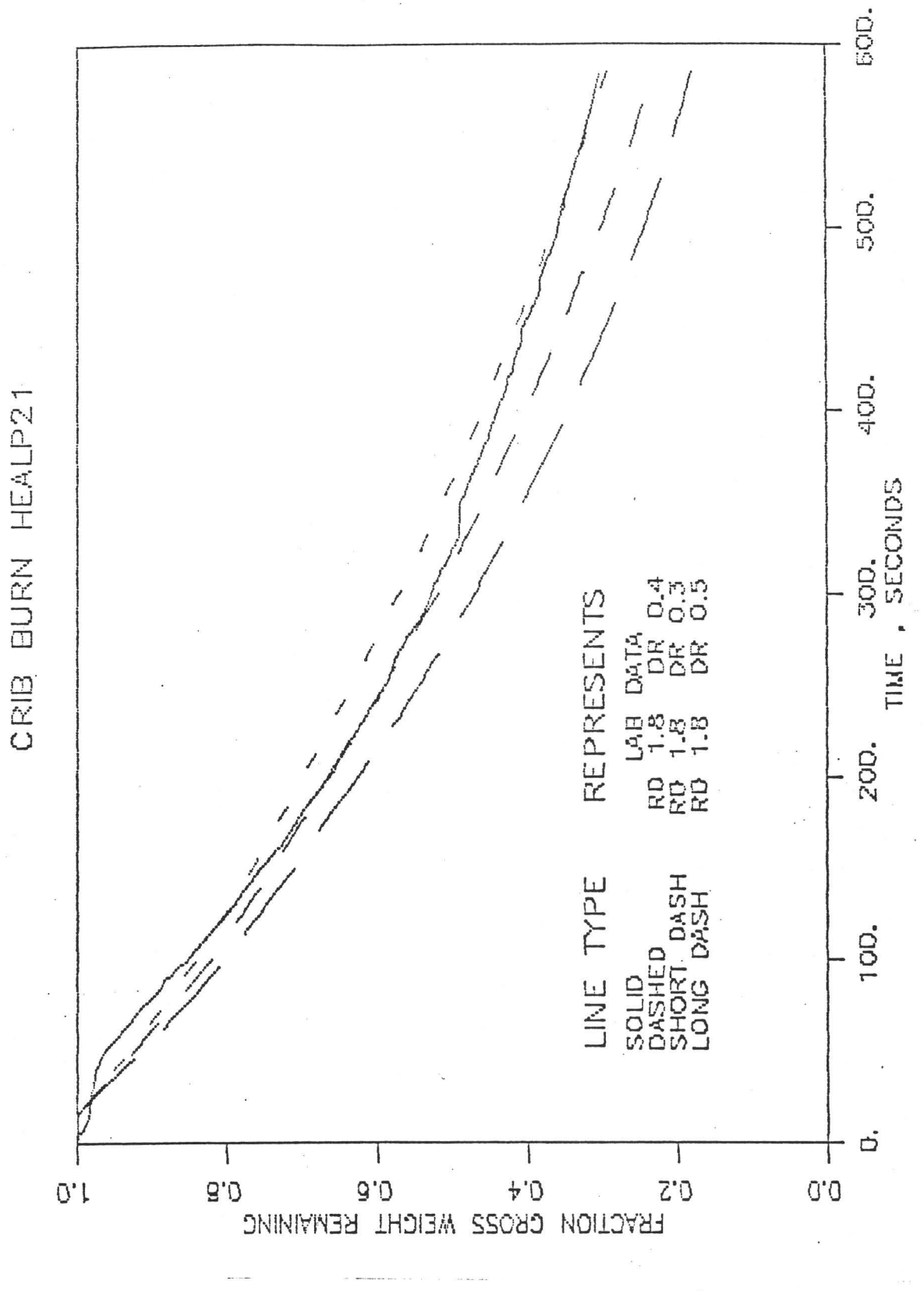

Fig. 2. Predicted burning rates for crib HEALP21 for r0 = 1.8 and three different values of dr, compared to the experimental record of weight as a function of time. By means of many such graphical comparisons, the "best" values of r0 and dr, 1.80 and 0.43 respectively, were selected.

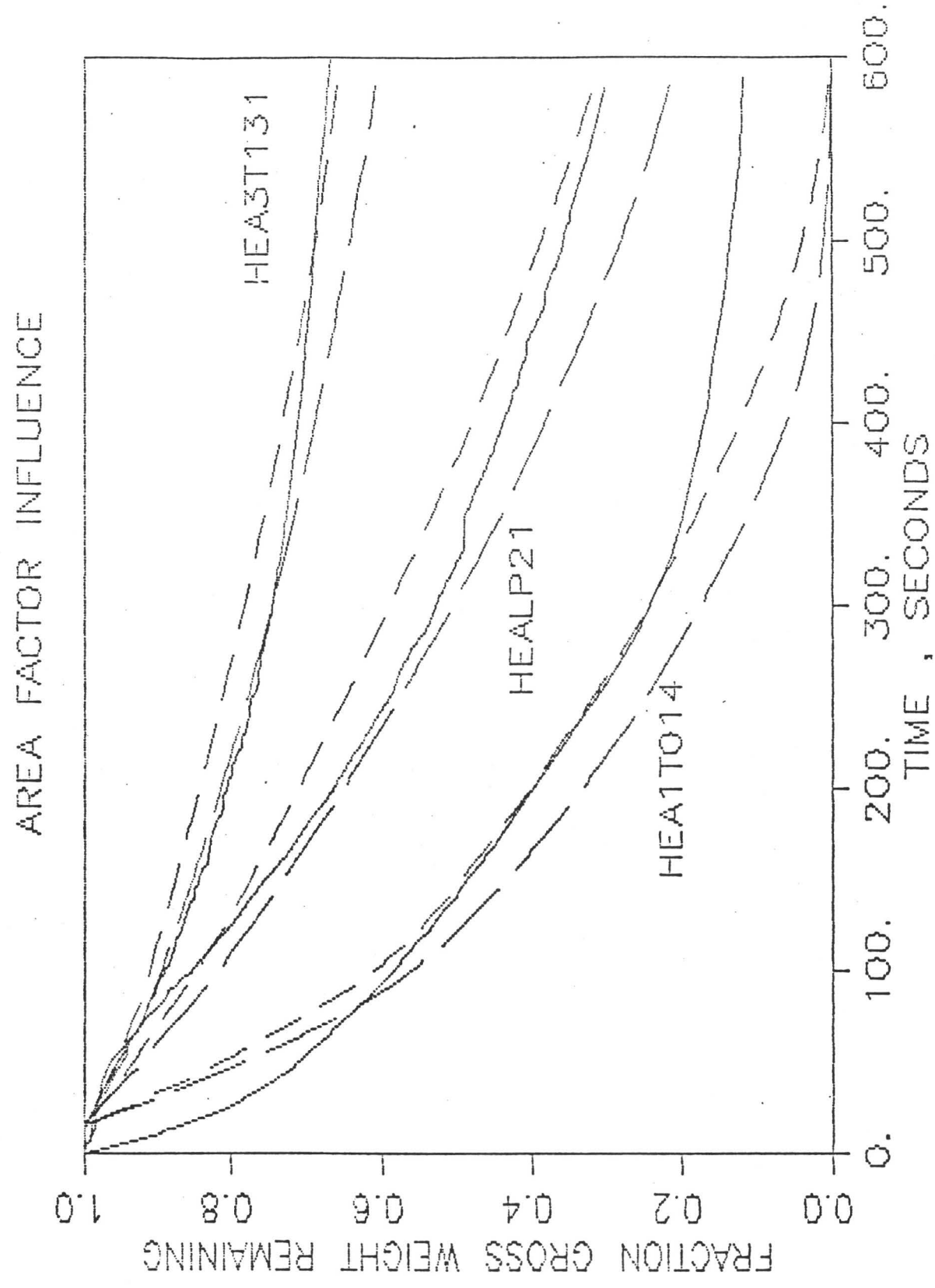

Fig. 3. Weight vs time (solid lines) for a 3.5 kg crib, HEA1TO14, a 44 kg crib, HEALP21, and a 200 kg crib, HEA3T131. Model predictions using area factors K_a = 2.50 (long dash) and 0.05 (short dash), and the "best" values for r0 and dr are shown for comparison.

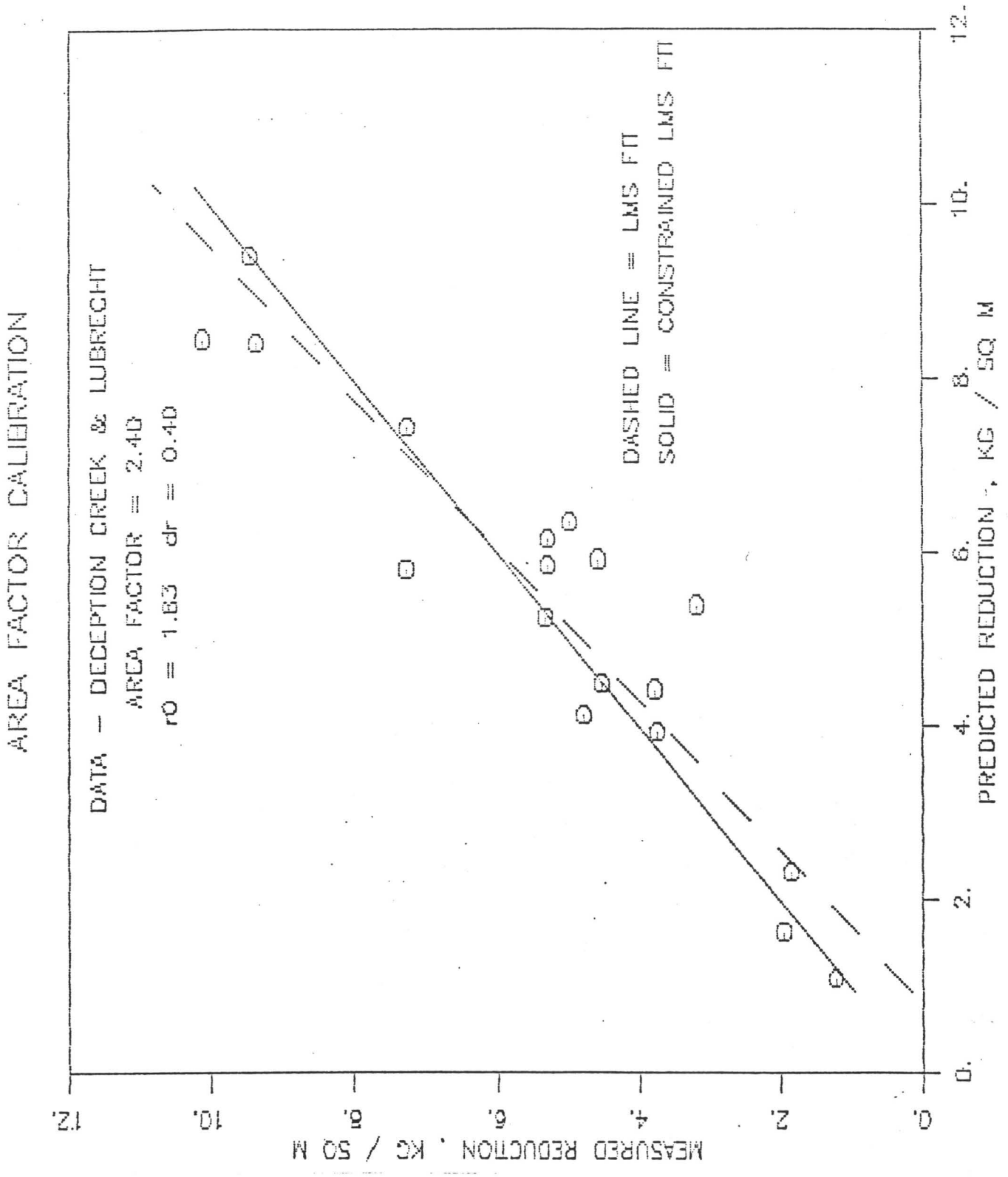

Fig. 4. Scatter plot of calibration exercise predictions and measurements of surface fuel loading reductions for 18 burn sites from data sets for Deception Creek and Lubrecht study areas. Two least squares linear fits are shown; the solid line is constrained to include the origin; the dashed line is not.

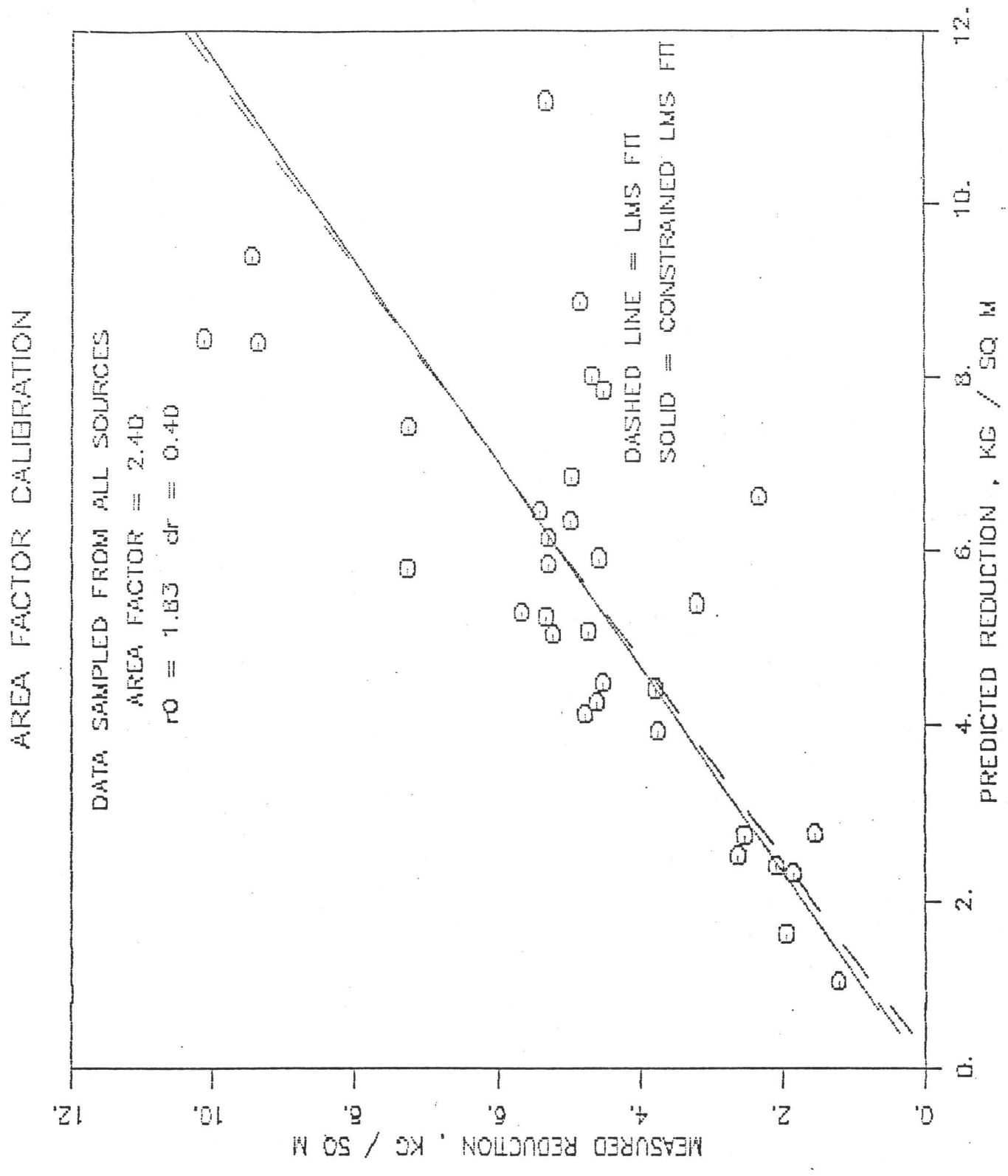

Fig. 5. Scatter plot of Fig. 4 with the addition of 15 burn sites from PNW study areas. Note the five severe overpredictions now included.

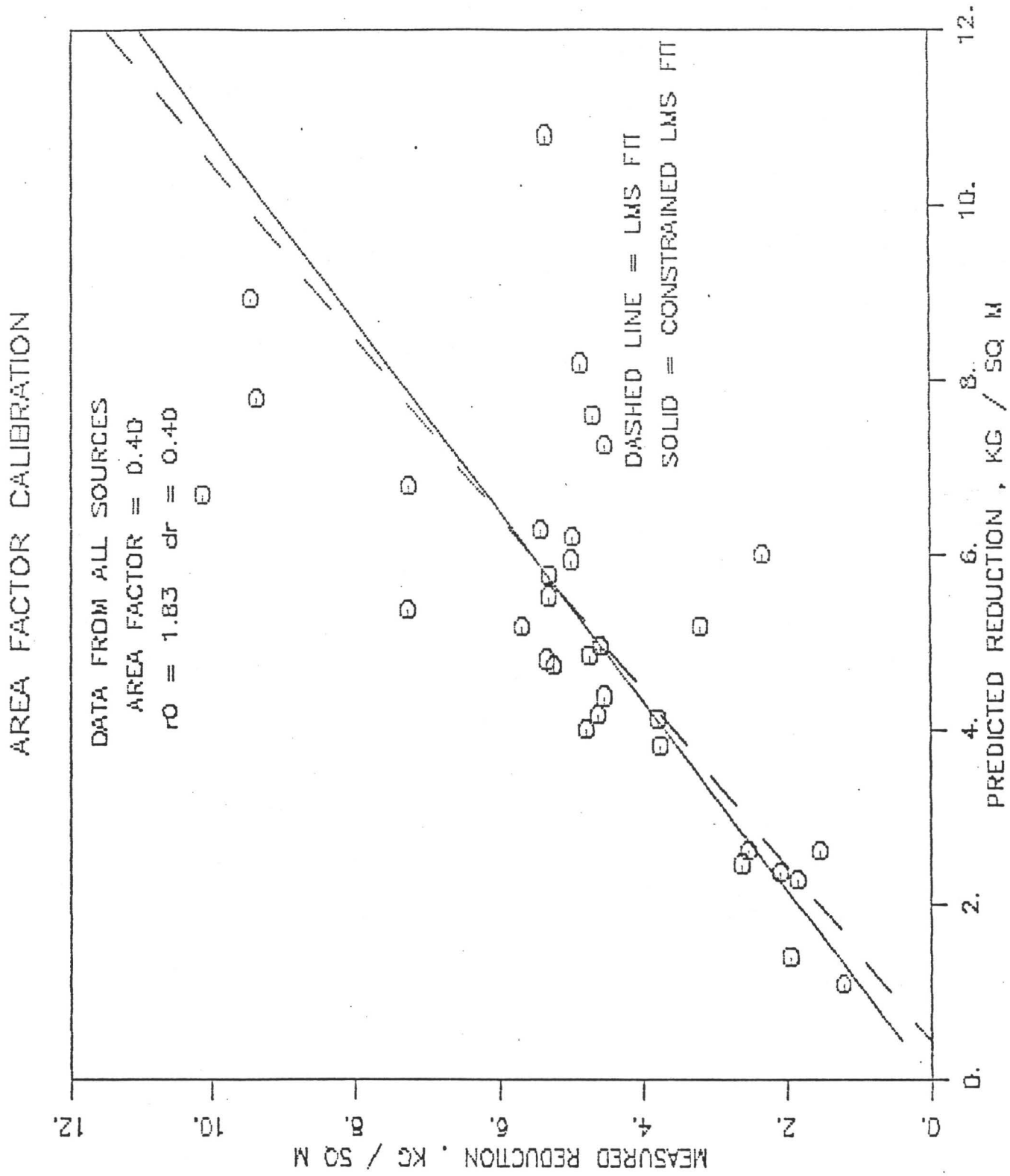

Fig. 6. Area factor calibration exercise shows acceptable surface fuel reduction predictions using area factor 0.4 and data from all study areas.

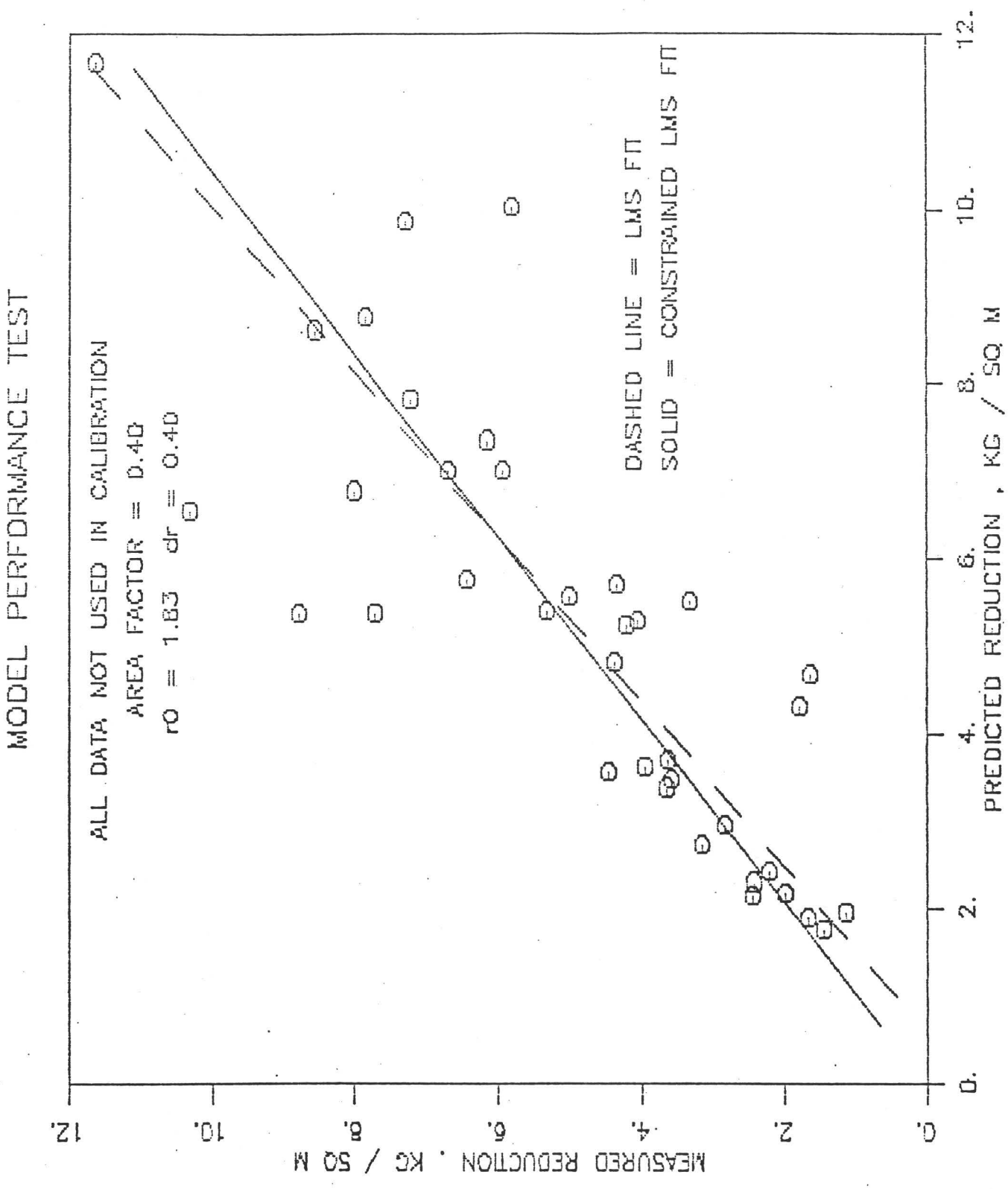

Fig. 7. Performance of the model in predicting surface fuel loading reductions for all sites excluded from the calibration exercises.

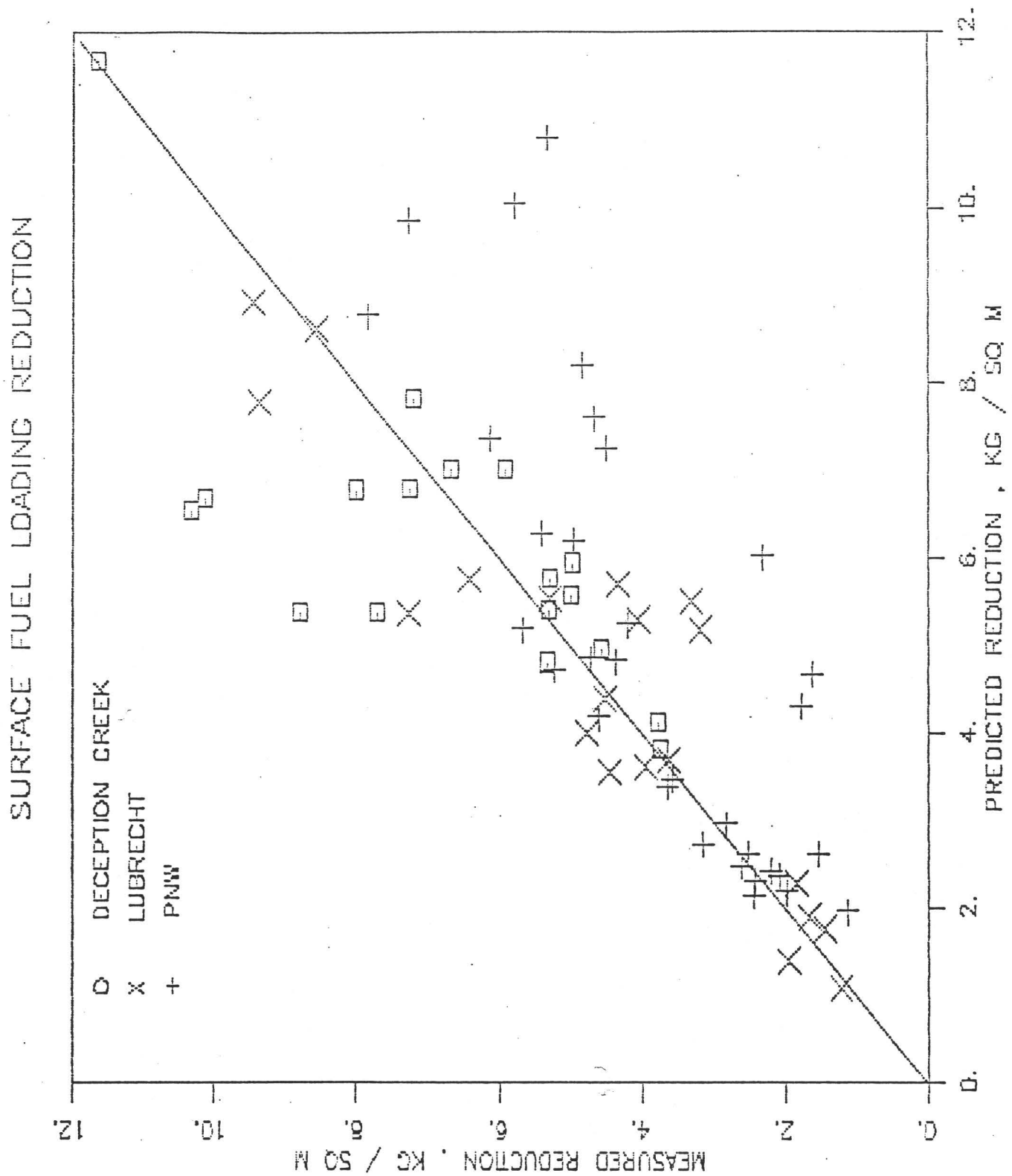

Fig. 8. Scatter plot superposition of Figs. 6 and 7, using different symbols for the three different study areas. Note underprediction of three Deception Creek units and overprediction of six to eight units from PNW data set.

REFERENCES

Albini, F. A., 1976: Computer-based models of wildland fire behavior: A users' manual. USDA Forest Service Unnumbered publication, Intermountain Research Station, Ogden UT. 68 pp.

Albini, F. A., 1981: Spot fire distance from isolated sources -- extensions of a predictive model. USDA Forest Service Research Note INT-309, Intermountain Research Station, Ogden UT. 9 pp.

Albini, F. A., 1986: Wildland fire spread by radiation -- a model including fuel cooling by natural convection. Combustion Science and Technology Volume 45, pp 101-113.

Albini, F. A., 1994: Program BURNUP, a simulation model of the burning of large woody natural fuels. Final report on USDA Forest Service Research Grant INT-92754-GR, Montana State University Mechanical Engineering Department. Unpublished report on file at USDA Forest Service Intermountain Fire Sciences Laboratory, Missoula MT.

Albini, Frank A., and Elizabeth D. Reinhardt, 1995: Modeling ignition and burning rate of large woody natural fuels. [In process]

Anderson, Hal E., 1990: Relationship of fuel size and spacing to combustion characteristics of laboratory fuel cribs. USDA Forest Service Research Paper INT-424, Intermountain Research Station, Ogden UT. 9 pp.

Andrews, P. L., 1986: BEHAVE: Fire behavior prediction and fuel modeling system -- BURN subsystem, part 1. USDA Forest Service General Technical Report INT-194. Intermountain Research Station, Ogden UT.

Andrews, P. L., and C. H. Chase, 1989: BEHAVE: Fire behavior prediction and fuel modeling system -- BURN subsystem, part 2. USDA Forest Service General Technical Report INT-260. Intermountain Research Station, Ogden UT.

Brown, Arthur A., and Kenneth P. Davis, 1973: Forest fire: Control and use, 2nd edition. McGraw-Hill, New York, 686 pp. See chapters 6 and 7.

Brown, J. K., M. A. Marsden, K. C. Ryan, and E. D. Reinhardt, 1985: Predicting duff and woody fuel consumption in the northern rocky mountains. USDA Forest Service Research Paper INT-337, Intermountain Research Station, Ogden UT. 23 pp.

Brown, James K., Elizabeth D. Reinhardt, and William C. Fischer, 1991: Predicting duff and woody fuel consumption in northern Idaho prescribed fires. Forest Science, Volume 37 Number 6 pp 1550-1566.

Chandler, C., P. Cheney, P. Thomas, L. Trabaud, and D. Williams, 1983: Fire in forestry. Volume 1, Forest fire behavior and effects. Wiley-Interscience, New York.

Drysdale, Dougal, 1985: An introduction to fire dynamics. John Wiley and Sons, Chichester. 424 pp. See chapter 5.

Frandsen, William H., 1991a: Burning rate of smoldering peat. Northwest Science, Volume 65 Number 4, pp 166-172.

Frandsen, William H., 1991b: Heat evolved from smoldering peat. International Journal of Wildland Fire, Volume 1 Number 3, pp 197-204.

Grishin, A. M., 1981: Matematicheskoye modeli lesnykh pozharov (Mathematical models of forest fires), Tomsk State University Press, Tomsk. 277 pp (Russian)

Grishin, A. M., 1992: Matematicheskoye modelirovaniye lesnykh pozharov i novyye sposoby bor'by s nimi (Mathematical modeling of forest fires and new methods of fighting them), Nauka, Novosibirsk. 408 pp. (Russian)

Harmathy, T. Z., 1972a: A new look at compartment fires, Part I. Fire Technology Volume 8 Number 3, pp 196-217.

Harmathy, T. Z., 1972b: A new look at compartment fires, Part II. Fire Technology Volume 8 Number 4, pp 326-354.

Hasemi, Y., and T. Tokunaga, 1983: Modeling of turbulent diffusion flames and fire plumes for the analysis of fire growth, pp 37-46 In Quintierre, J. G., R. L. Alpert, and R. A. Altenkirch (editors), "Fire dynamics and heat transfer", Annals of American Society of Mechanical Engineers, Heat Transfer Division, HTD-Volume 25. ASME, New York, 138 pp.

Heskestad, Gunnar 1991: A reduced-scale mass fire experiment. Combustion and Flame, Volume 83, pp 293-301.

Hungerford, Roger D., 1990: Describing downward heat flow for predicting fire effects. Problem analysis, problem no. 1, addendum, 7/9/90, Research Work Unit FS-INT-4403, Fire effects: Prescribed and wildfire. USDA Forest Service Intermountain Research Station, Intermountain Fire Sciences Laboratory, Missoula MT. 100 pp.

Incropera, Frank P. and David P. DeWitt, 1985: "Fundamentals of heat and mass transfer", second edition. John Wiley & Sons, New York, 802 pp. Section 7.4.2.

Luke, R. H., and A. G. McArthur, 1977: Bushfires in Australia, Australian Government Publishing Service, Canberra, 359 pp. See Chapters 4 and 6.

Norum, Rodney A., 1975: Characteristics and effects of understory fires in western larch/Douglas-fir stands. Ph.D. dissertation, University of Montana School of Forestry, Missoula MT. 155 pp.

Norum, Rodney A., 1976: Fire intensity-fuel reduction relationships associated with understory burning in larch/Douglas-fir stands. pp 559-572 In: Proceedings Tall Timbers fire ecology conference no. 14 and Intermountain Fire Research Council fire and land management symposium, October 1974, Missoula MT. Tallahassee FL: Tall Timbers Research Station.

Reinhardt, Elizabeth D., James K. Brown, William C. Fischer, and Russel T. Graham, 1991: Woody fuel and duff consumption by prescribed fire in northern Idaho mixed conifer

logging slash. USDA Forest Service Research Paper INT-443 Intermountain Research Station, Ogden UT. 22 pp.

Rothermel, R. C., 1972: A mathematical model for predicting fire spread in wildland fuels. USDA Forest Service Research Paper INT-115, Intermountain Research Station, Ogden UT. 40 pp.

Sandberg, D. V., and R. D. Ottmar, 1983: Slash burning and fuel consumption in the Douglas-fir subregion, pp 90-93 in: Seventh conference on fire and forest meteorology, American Meteorological Society, Boston MA.

RULES FOR SELECTION OF MIXING PARAMETER
AND CALCULATION OF LOCAL FIRE INTENSITY

Case	Component ignited?	Size category of interaction partner	Fraction partner category ignited	Mixing parameter r	Local fire intensity I
1	No	None	---	r_0	$I_f + I_d$
2	No	Own = k	0	r_0	I_f
3	No	Smaller = j	f_j	$r_0 + 0.5f_j dr$	$I_f + f_j I_j$
4	Yes	None	---	$r_0 + 0.5dr$	$I_f + I_d$
5	Yes	Own = k	f_k	$r_0 + 0.5(1+f_k)dr$	$I_f + f_k I_k$
6	Yes	Smaller = j	f_j	$r_0 + 0.5(1+f_j)dr$	$I_f + I_k + f_j I_j$

Table 1. Rules for selection of mixing parameter and calculation of local fire intensity. I_f is the site-average fire intensity, I_d the site-average intensity due to duff burning, and I_j, I_k are incremental local intensities due to burning of interacting fuel elements of categories j and k. Fuel component k,j of category k is being considered in this table. If the interaction partner category (j) of this component is ignited, it contributes an incremental intensity I_j to its local fire environment with probability f_j

BURN NUMBER	DRY FUEL WEIGHT, kg	FINE FUEL LOAD FRACTION EXCELSIOR	1/4 IN	MOISTURE FRACTION
CRIBS WITH BURNING RATES LIMITED BY FUEL SURFACE AREA EXPOSED				
HEALP41	32.1	.00825	.0444	.060
HEAPP41	32.1	.00848	.0482	.067
HEALP21	44.1	.00720	.0431	.065
HEASF21	45.7	.00695	.0416	.065
HEALP31	51.3	.00531	.0353	.065
HEADF21	57.4	.00712	.0420	.065
HEAPP31	61.4	.00296	.0289	.060
HEASF41	72.0	.00692	.0422	.060
HEA2T111	78.3	.00973	.0913	.060
HEALP51	98.9	.00550	.0367	.060
HEAPP61	102.1	.00444	.0307	.060
HEADF41	103.4	.00702	.0378	.060
HEAPP101	106.5	.00681	.0341	.080
HEA2T061	159.3	.00683	.111	.060
HEAPP71	161.5	.00444	.0307	.060
HEA3T131	199.6	.00496	.0363	.060
CRIBS WITH BURNING RATES INITIALLY LIMITED EQUALLY BY TOP SURFACE VENT AREA AND BY FUEL SURFACE AREA EXPOSED				
HEAPP21	46.3	.00686	.0420	.060
HEADF31	81.1	.00279	.0291	.060
HEA3T161	81.2	.00559	.0392	.050
HEADF51	152.4	.00324	.0260	.137
HEADF52	152.4	.00324	.0260	.220
HEA3T151	188.7	.00461	.0331	.050
CRIBS WITH BURNING RATES LIMITED BY TOP SURFACE VENT AREA				
HEASF31	82.0	.00205	.0230	.117
HEALP61	95.9	.00180	.0235	.225
HEASF51	161.0	.00176	.0206	.060
HEAPP81	163.7	.00298	.0241	.060
HEAPP91	217.7	.00204	.0213	.060
HEA3T141	235.0	.00399	.0269	.060
CRIBS WITH BURNING RATE LIMITS NOT DETERMINED				
HEA1T014	3.5	.0284	.227	.060
HEA3T171	23.9	.0830	.236	.060
HEA1T015	25.5	.0375	.241	.060
HEA3T173	25.5	.0781	.222	.060
HEA3T172	28.3	.0703	.200	.060

Table 2. Characteristics of the laboratory wood cribs whose burning rates were used to select the best mixing parameters r0 and dr for the simulation.

CRIB FUEL LOADING DISTRIBUTIONS BY SIZE: EXCELSIOR PLUS SQUARE CROSS SECTION DIMENSIONED LUMBER (DIMENSIONS IN INCHES)

BURN	LOADING, kg (DRY WEIGHT) / m^2					
NUMBER	EXCELSIOR	1/4 x 1/4	1 x 1	2 x 2	4 x 4	6 x 6
HEA1T014	.437	4.30	14.1			
HEA1T015	.644	4.13	12.4			
HEA2T061	.732	11.9	30.9		63.6	
HEA2T111	.513	4.79	13.5	33.9		
HEA3T131	.668	4.89	14.1			115.
HEA3T141	.632	4.27	12.5			141.
HEA3T151	.586	4.21	12.3		110.	
HEA3T161	.305	2.14	8.54	43.6		
HEA3T171	1.34	3.81	11.0			
HEA3T172	1.34	3.81	13.9			
HEA3T173	1.34	3.81	12.0			
HEADF21	.275	1.62	5.61	31.1		
HEADF31	.166	1.73	6.01	51.5		
HEADF41	.532	2.86	8.97		63.4	
HEADF51	.397	3.18	9.94		109.	
HEADF52	.397	3.18	9.94		109.	
HEALP21	.214	1.28	4.33	23.9		
HEALP31	.191	1.27	4.30	30.2		
HEALP41	.532	2.86	8.97		52.1	
HEALP51	.436	2.91	9.08		66.8	
HEALP61	.121	1.58	5.44	60.1		
HEAPP101	.488	2.44	7.72			61.0
HEAPP21	.214	1.31	4.55	25.1		
HEAPP31	.133	1.30	4.55	39.0		
HEAPP41	.239	1.36	4.78	21.8		
HEAPP51	.465	2.56	9.74		57.0	
HEAPP61	.363	2.51	7.77		71.1	
HEAPP71	.763	3.63	11.1			93.1
HEAPP81	.430	3.48	10.6			130.
HEAPP91	.326	3.39	10.1			146.
HEASF21	.214	1.28	4.49	24.8		
HEASF31	.118	1.32	4.57	51.5		
HEASF41	.483	2.94	9.36		57.0	
HEASF51	.206	2.42	7.60		107.	

Table 3. Distributions of fuel size categories for the laboratory wood cribs used in burning rate calibration trials.

RESULTS OF MODEL CALIBRATION TRIAL EXERCISES
TO SELECT THE BEST VALUE OF AREA FACTOR K_a

				K_a				
				0.6	1.2	1.8	2.4	3.0
Study area	Burns	Load Reductions Mean	Std Dev	------- Mean errors of prediction ------- -- Mean squared errors of prediction --				
Deception Creek	8	5.63	1.98	-0.19 1.54	0.02 1.16	0.20 1.00	0.36 0.97	0.50 1.02
Lubrecht	10	4.88	2.84	-0.25 1.11	-0.17 1.01	-0.10 0.94	-0.03 0.89	0.03 0.87
PNW	15	4.06	1.36	1.40 5.18	1.49 5.61	1.58 6.10	1.67 6.58	1.75 7.05
Lubrecht & Deception Creek	18	5.21	2.53	-0.23 1.30	-0.09 1.08	0.03 0.97	0.14 0.93	0.24 0.94
All Sources	33	4.69	2.16	0.51 3.06	0.63 3.14	0.74 3.30	0.84 3.50	0.93 3.72

Table 4. Results of calibration exercises of the simulation to predict fuel consumption in prescribed burns in three locales. Mean and standard deviation of surface fuel loading reductions are given in kg/m^2, along with mean errors of prediction and mean squared errors of prediction in the same units.

MEASURES OF THE DEGREE TO WHICH MODEL PREDICTIONS FIT CALIBRATION DATA FOR SELECTING BEST VALUE OF AREA FACTOR

Study area	Burns	K_a	1 - MSE/VAR	Linear fits to scatter plots a	b	c
		0.60	0.609	-5.39	2.03	1.08
Deception		1.20	0.706	-4.25	1.75	1.04
Creek	8	1.80	0.746	-3.62	1.59	1.00
		2.40	0.754	-3.20	1.47	0.97
		3.00	0.741	-2.88	1.39	0.95
		0.60	0.863	-0.56	1.18	1.08
		1.20	0.875	-0.54	1.15	1.06
Lubrecht	10	1.80	0.884	-0.50	1.13	1.04
		2.40	0.890	-0.48	1.10	1.03
		3.00	0.892	-0.45	1.09	1.01
		0.60	-1.800	1.61	0.45	0.71
		1.20	-2.032	1.64	0.44	0.70
PNW	15	1.80	-2.297	1.68	0.42	0.68
		2.40	-2.557	1.73	0.41	0.67
		3.00	-2.811	1.76	0.40	0.66
		0.60	0.796	-1.24	1.29	1.08
Lubrecht &		1.20	0.831	-1.13	1.24	1.05
Deception	18	1.80	0.848	-1.04	1.19	1.02
Creek		2.40	0.854	-0.96	1.15	1.00
		3.00	0.853	-0.89	1.12	0.98
		0.60	0.342	-0.42	0.98	0.91
		1.20	0.325	-0.35	0.95	0.89
All Sources	33	1.80	0.290	-0.26	0.91	0.87
		2.40	0.247	-0.19	0.88	0.85
		3.00	0.200	-0.12	0.86	0.84

Table 5. Measures of the degree to which model predictions fit measurements of surface fuel loading reduction for three prescribed burn study locales. The second column gives values of a measure of model error, defined to be 1 - (mean squared error of prediction) / (variance of observations). Parameters a and b are intercept and slope of a least squares best fit of a straight line graphing observations against predictions. Parameter c is the slope of the same best fit line if it is constrained to pass through the origin.

MEASURES OF THE DEGREE TO WHICH MODEL PREDICTIONS FIT MEASUREMENT DATA FOR SELECTION AND TEST OF AREA FACTOR

Study area	Burns	K_a	1 - MSE/VAR	Linear fits to scatter plots a	b	c
		0.10	0.338	-0.46	1.01	0.93
Calibration		0.20	0.340	-0.45	1.00	0.93
data set -	33	0.30	0.342	-0.45	1.00	0.92
all sources		0.40	0.342	-0.44	0.99	0.92
		0.50	0.342	-0.43	0.99	0.91
Test set		0.10	0.648	-0.74	1.10	0.98
(all data		0.20	0.646	-0.71	1.08	0.97
excluded	37	0.30	0.643	-0.68	1.07	0.96
from		0.40	0.643	-0.65	1.06	0.96
calibration)		0.50	0.640	-0.62	1.05	0.95
		0.10	0.411	-2.67	1.56	1.14
Deception		0.20	0.431	-2.58	1.53	1.13
Creek	18	0.30	0.451	-2.49	1.50	1.12
		0.40	0.468	-2.43	1.48	1.11
		0.50	0.484	-2.35	1.46	1.10
		0.10	0.825	-0.68	1.15	1.03
		0.20	0.825	-0.68	1.14	1.02
Lubrecht	20	0.30	0.827	-0.67	1.14	1.02
		0.40	0.827	-0.67	1.14	1.02
		0.50	0.828	-0.66	1.13	1.02
		0.10	-0.229	0.77	0.62	0.75
		0.20	-0.253	0.78	0.62	0.75
PNW	32	0.30	-0.273	0.79	0.61	0.74
		0.40	-0.294	0.80	0.61	0.74
		0.50	-0.317	0.80	0.61	0.74
		0.10	0.531	-0.66	1.07	0.96
		0.20	0.531	-0.64	1.06	0.95
ALL DATA	70	0.30	0.529	-0.61	1.05	0.94
		0.40	0.529	-0.59	1.04	0.94
		0.50	0.528	-0.57	1.03	0.94

Table 6. Presents the same measures of goodness of fit as in Table 5, but using only data not included in the calibration trials (second block) and using all data (last four blocks). The range of values for K_a is much smaller in this table than in Table 5 also.

$$q_{net}'' = h_{eff}(T_F - T_S). \quad (1)$$

$$Q_c'' = \rho U C_p (T_F - T_a), \quad (2)$$

$$Q_r'' = \varepsilon \sigma (T_F^4 - T_a^4), \quad (3)$$

$$Q_c'' + Q_r'' = I. \quad (4)$$

$$\rho U = (1 + \Phi) I / H_c \quad (5)$$

$$\theta = 1 + r / (1 + A r (\theta + 1)(\theta^2 + 1) / I) \quad (6)$$

$$\theta = T_F / T_a, \quad (7)$$

$$A = \varepsilon \sigma T_a^4, \quad (8)$$

$$r = H_c / ((1 + \Phi) C_p T_a) \quad (9)$$

$$\max(T_F) = (1 + r) T_a, \quad (10)$$

$$b_{ij} = K_a \sigma_j w''_i / \rho_i \pi \quad (11)$$

$$b_{ij} = (D_i / D_j) b_{ii} \quad (12)$$

$$b_{ij} = \min(1 , b_{ij}) \quad (13)$$

$$\beta_{jj} = 1 - \exp(- b_{jj}). \quad (14)$$